



RESEARCH ARTICLE

REVISED Molecular signature of anastasis for reversal of apoptosis
[version 2; referees: 3 approved]

Ho Man Tang¹, C. Conover Talbot Jr¹, Ming Chiu Fung², Ho Lam Tang ³

¹Institute for Basic Biomedical Sciences, Johns Hopkins University School of Medicine, Baltimore, USA

²School of Life Sciences, Chinese University of Hong Kong, Shatin, Hong Kong

³W. Harry Feinstone Department of Molecular Microbiology and Immunology, Johns Hopkins University Bloomberg School of Public Health, Baltimore, USA

v2 First published: 13 Jan 2017, 6:43 (doi: [10.12688/f1000research.10568.1](https://doi.org/10.12688/f1000research.10568.1))
Latest published: 09 Feb 2017, 6:43 (doi: [10.12688/f1000research.10568.2](https://doi.org/10.12688/f1000research.10568.2))

Abstract

Anastasis (Greek for "rising to life") is a cell recovery phenomenon that rescues dying cells from the brink of cell death. We recently discovered anastasis to occur after the execution-stage of apoptosis *in vitro* and *in vivo*. Promoting anastasis could in principle preserve injured cells that are difficult to replace, such as cardiomyocytes and neurons. Conversely, arresting anastasis in dying cancer cells after cancer therapies could improve treatment efficacy. To develop new therapies that promote or inhibit anastasis, it is essential to identify the key regulators and mediators of anastasis – the therapeutic targets. Therefore, we performed time-course microarray analysis to explore the molecular mechanisms of anastasis during reversal of ethanol-induced apoptosis in mouse primary liver cells. We found striking changes in transcription of genes involved in multiple pathways, including early activation of pro-cell survival, anti-oxidation, cell cycle arrest, histone modification, DNA-damage and stress-inducible responses, and at delayed times, angiogenesis and cell migration. Validation with RT-PCR confirmed similar changes in the human liver cancer cell line, HepG2, during anastasis. Here, we present the time-course whole-genome gene expression dataset revealing gene expression profiles during the reversal of apoptosis. This dataset provides important insights into the physiological, pathological, and therapeutic implications of anastasis.

Open Peer Review

Referee Status:

	Invited Referees		
	1	2	3
REVISED			
version 2	report		report
published			
09 Feb 2017			
version 1			
published	report	report	
13 Jan 2017			

- 1 **Takafumi Miyamoto**, University of Tokyo
Japan
- 2 **Sanzhen Liu**, Kansas State University
USA
- 3 **Leonard K. Kaczmarek**, Yale School of
Medicine USA

Discuss this article

Comments (0)

Corresponding authors: Ho Man Tang (homantang@jhmi.edu), Ming Chiu Fung (mingchiufung@cuhk.edu.hk), Ho Lam Tang (holamtang@jhmi.edu)

How to cite this article: Tang HM, Talbot Jr CC, Fung MC and Tang HL. **Molecular signature of anastasis for reversal of apoptosis [version 2; referees: 3 approved]** *F1000Research* 2017, **6**:43 (doi: [10.12688/f1000research.10568.2](https://doi.org/10.12688/f1000research.10568.2))

Copyright: © 2017 Tang HM *et al.* This is an open access article distributed under the terms of the [Creative Commons Attribution Licence](#), which permits unrestricted use, distribution, and reproduction in any medium, provided the original work is properly cited. Data associated with the article are available under the terms of the [Creative Commons Zero "No rights reserved" data waiver](#) (CC0 1.0 Public domain dedication).

Grant information: This work was supported by the Shurl and Kay Curci Foundation of the Life Sciences Research Foundation fellowship (H.L.T.).

The funders had no role in study design, data collection and analysis, decision to publish, or preparation of the manuscript.

Competing interests: No competing interests were disclosed.

First published: 13 Jan 2017, **6**:43 (doi: [10.12688/f1000research.10568.1](https://doi.org/10.12688/f1000research.10568.1))

REVISED Amendments from Version 1

In the revised manuscript, we have added new data that support our conclusions. Specifically, our RT-PCR reveals that a human liver cancer cell line displays similar gene expression profile during anastasis as observed in mouse primary liver cells. Additional microarray statistical analysis is included as supplementary data. We have also discussed the potential molecular mechanisms, physiological and pathological consequences, and therapeutic potentials of anastasis.

See referee reports

Introduction

Apoptosis (Greek for “falling to death”) is essential for normal development and homeostasis of multicellular organisms by eliminating unwanted, injured, or dangerous cells^{1–3}. This cell suicide process was generally assumed to be irreversible because it involves rapid and massive cell destruction^{4–9}. During apoptosis, intrinsic and extrinsic pro-apoptotic signals can converge at mitochondria, leading to mitochondrial outer membrane permeabilization (MOMP), which releases cell execution factors, such as cytochrome *c* to trigger activation of apoptotic proteases including caspase-3 and -7^{10,11}, small mitochondria-derived activator of caspases (Smac)/direct IAP binding protein with low pI (DIABLO) to eliminate inhibitor of apoptosis protein (IAP) which suppresses caspase activation^{12,13}, and apoptosis-inducing factor (AIF) and endonuclease G to destroy DNA^{14–17}. Activated caspases commit cells to destruction by cleaving hundreds of functional and structural cellular substrates^{4,18}. Crosstalk between signalling pathways amplifies the caspase cascade to mediate cell demolition via nucleases (DNA fragmentation factor [DFF]/caspase-activated DNase [CAD]) to further destroy the genome^{19–21}, and alter lipid modifying enzymes to cause membrane blebbing and apoptotic body formation^{22,23}. Therefore, cell death is considered to occur after caspase activation within a few minutes^{24–26}.

However, we and other groups have demonstrated reversal of early stage apoptosis, such as externalization of phosphatidylserine (PS) in cultured primary cells and cancer cell lines^{27–30}. We have further demonstrated that dying cells can reverse apoptosis even after reaching the generally assumed “point of no return”^{29–31}, such as MOMP-mediated cytochrome *c* release, caspase-3 activation, DNA damage, nuclear fragmentation, and apoptotic body formation^{4–9}. Our observation of apoptosis reversal at late stages is further supported by an independent study, which shows recovery of cells after MOMP³². To detect reversal of apoptosis in live animals, we have further developed a new *in vivo* caspase biosensor, designated “CaspaseTracker”³³, to identify and track somatic, germ and stem cells that recover after transient cell death inductions, and also potentially during normal development and homeostasis in *Drosophila melanogaster* after caspase activation^{33,34}, the hallmark of apoptosis^{4,35}. We proposed the term “anastasis”³⁰, which means “rising to life” in Greek, to describe this recovery from the brink of cell death. Anastasis appears to be an intrinsic cell survival phenomenon, as removal of cell death stimuli is sufficient to allow dying cells to recover^{29–31,33}.

The physiological, pathological and therapeutic importance of anastasis is not yet known. We proposed that anastasis could be an unexpected tactic that cancer cells use to escape cancer therapy^{29–31}. Many tumours undergo dramatic initial responses to cell death-inducing radiation or chemotherapy^{36–39}; however, these cells relapse, and metastasis often occurs in most types of cancer^{36–39}. Therefore, the ability of cells to recover from transient induction of cell death may allow tumour cells to escape treatment, and survive and proliferate, resulting in relapse^{29–31}. Furthermore, cells may acquire new oncogenic mutations and transformation phenotypes during anastasis^{30,31}, such as DNA damage caused by apoptotic nucleases. Therefore, anastasis could be one of the mechanisms underlying the observation that repeated tissue injury increases the risk of cancer in a variety of tissues⁴⁰, such as liver damage due to alcoholism⁴¹, chronic thermal injury in the oesophagus induced by the consumption of very hot beverages^{42–44}, evolution of drug resistance in recurrent cancers^{36–39,45}, and development of a second cancer during subsequent therapy^{46–49}. Anastasis can also occur in primary cardiac cells and neuronal cell lines^{30,31}, and potentially in cardiomyocytes *in vivo* following transient ischemia⁵⁰. These findings suggest anastasis as an unexpected cellular protective mechanism. Therefore, uncovering the mechanisms of anastasis may provide new insights into the regulation of cell death and survival, and harnessing this mechanism via suppression or promotion of anastasis would aid treatment of intractable diseases including cancer, heart failure and neurodegeneration.

Our previous study demonstrated reversibility of ethanol-induced apoptosis at late stages in mouse primary liver cells, and revealed that new transcription is important to reverse apoptosis^{30,31}. During recovery, we found up-regulation of genes involved in pro-survival pathways and DNA damage responses during anastasis (Bag3, Mcl1, Dnajb1, Dnajb9, Hsp90aa1, Hspa1b, and Hspb1, Mdm2)³⁰. Interestingly, inhibiting some of those genes by corresponding specific chemical inhibitors significantly suppresses anastasis³⁰. However, the molecular mechanism of anastasis remains to be elucidated. To study the cellular processes of anastasis, we performed time-course RNA microarray analysis to determine the gene expression profiles of the cultured mouse primary liver cells undergoing anastasis following transient exposure to ethanol that triggers apoptosis, and identified unique gene expression patterns during reversal of apoptosis. We also performed reverse transcription polymerase chain reaction (RT-PCR) to validate the gene expression patterns in the human liver cancer cell line, HepG2, during anastasis. Here, we present our time-course microarray data, which reveals the molecular signature of anastasis.

Methods

Microarray

Mouse primary liver cells were isolated from BALB/c mice using collagenase B and cultured as described^{30,51}. The cells were cultured in DMEM/F-12 (DMEM:nutrient mixture F-12) supplemented with 10% fetal bovine serum (FBS), 100 U/ml penicillin, and 100 µg/ml streptomycin (Life Technologies, Carlsbad, CA, USA) at 37°C under an atmosphere of 5% CO₂/95% air. To induce apoptosis, cells were exposed to 4.5% ethanol for 5 hours (RO) in

the culture medium (vol/vol). To allow recovery, dying cells were washed and further incubated in the fresh culture medium for 3 hours (R3), 6 hours (R6), 24 hours (R24), and 48 hours (R48). The untreated cells served as control (Ctrl). Three biological replicates were performed at each time point. Total RNA in the corresponding cell conditions was harvested using TRIzol Reagent (Life Technologies). The RNA was purified using the RNeasy Mini Kit (Qiagen, Cologne, Germany). Reverse transcription was performed using SABiosciences C-03 RT² First Strand Kit to construct cDNA (SABiosciences-Qiagen, Frederick, MD, USA). The cDNA samples were analysed using the Illumina MouseWG-6 v2.0 Expression BeadChip (Illumina, San Diego, CA, USA).

Gene expression data analysis

The Partek Genomics Suite 6.6 (Partek, St. Louis, MO, USA) was used for principal component analysis (PCA)^{52,53}. The Spotfire DecisionSite 9.1.2 (TIBCO, Palo Alto, CA, USA) platform was used to evaluate the fold change of gene expression levels between time points when compared with a common starting point, which is the control (Ctrl)⁵⁴. Signal values were converted into log₂ space and quality control tests were performed to ensure data integrity by comparing the signals of the three biological replicates at each time point. The fold change was based on averaged values of the three replicates at each time point; two-sample Student's *t*-test was used to determine statistical significance as *p*-values of less than 0.05, using the Partek Genomics Suite v6.5 (Partek Inc., St. Louis, MO, USA).

For the time-course gene expression analysis using Spotfire, all time points were compared with the time point Ctrl, which represents untreated cells. Spotfire was used to show the genes that displayed specific changes in gene expression after removal of cell death inducer for 3 hours (R3) and 6 hours (R6). Genes with specific and significant change (Log₂ > 1 or < -1) in expression at the corresponding timepoint are highlighted. Interaction network analysis of the up-regulated genes during anastasis was performed using the GeneMANIA database (<http://genemania.org/>)^{55,56}.

Confocal microscopy

Cells were incubated with 50 nM Mitotracker Red CMXRos and 250 ng/ml Hoechst 33342 (Invitrogen) for 20 minutes in culture medium to stain mitochondria and nuclei, respectively. The stained cells were washed and incubated with culture medium for 10 minutes, and then were fixed with 3.7% (wt/vol) paraformaldehyde in phosphate-buffer saline (PBS) solution for 20 minutes at room temperature in dark. The fixed cells were mounted on glass slide using ProLong Diamond Antifade Mountant (Invitrogen). Cell images were captured with the Zeiss LSM 780 confocal inverted microscope using a 40×, numerical aperture (NA) 1.4 plan-Apochromat objective (Carl Zeiss, Jena, Germany), and were analyzed using Zen 2013 or AxioVision 4.2 software (Carl Zeiss).

Reverse transcription polymerase chain reaction (RT-PCR)

Human liver cancer cell line HepG2 (ATCC HB-8065) was cultured in DMEM/F-12, 10% FBS, 100 U/ml penicillin, and 100 µg/ml streptomycin (Life Technologies) at 37°C under an atmosphere of 5% CO₂/95% air. Apoptosis was induced by incubation

of the cells with 4.5% ethanol in cell culture medium for 5 hours (R0). Then, the apoptotic dying cells were washed and then incubated in the fresh culture medium for 1 hour (R1), 2 hours (R2), 3 hours (R3), 4 hours (R4), 6 hours (R6), 9 hours (R9), 12 hours (R12), and 24 hours (R24). The untreated cells served as control (Ctrl). Total RNA in the corresponding cell conditions was harvested using QIAzol lysis reagent (Qiagen). The total RNA was purified using the RNeasy Mini Kit (Qiagen). Reverse transcription was performed using the SuperScript IV reverse transcriptase system (Thermo Fisher Scientific, Waltham, MA, USA). Primer sets for detecting targeted genes were designed using the Universal ProbeLibrary (Roche Applied Science, Madison, WI). Primer set for MMP10 was previously designed⁵⁷. Polymerase Chain Reaction (PCR) was performed using Taq DNA Polymerase and PCR protocol (New England BioLabs, Ipswich, MA, USA), with initial denaturation at 95°C for 2 minutes, followed by 30 cycles of denaturation at 95°C for 30 seconds, annealing at 60°C for 30 seconds, and extension at 72°C for 3 seconds. Electrophoresis of PCR products was performed using 4% agarose gel.

Results and discussion

We have demonstrated that mouse primary liver cells can reverse the apoptotic process at the execution stage^{30,31}, despite reaching important checkpoints commonly believed to be the “point of no return”⁴⁻⁹, including caspase-3 activation, DNA damage, and cell shrinkage. To pursue the mechanisms of anastasis, we performed time-course high-throughput microarray to evaluate gene expression profiles during reversal of ethanol-induced apoptosis in mouse primary liver cells. RNA samples were collected from the untreated primary liver cells (Ctrl), the cells treated with 4.5% ethanol for 5 hours when cells exhibited hallmarks of apoptosis (R0), and the treated cells that were then washed and cultured in fresh medium for 3 (R3), 6 (R6), 24 (R24) and 48 (R48) hours. Apoptosis was confirmed in the ethanol-treated cells (R0), which displayed hallmarks of apoptosis, including plasma membrane blebbing, cell shrinkage, cleavage of caspase-3 and its substrates, such as PARP and ICAD (Figure 1A and B, images reprinted with permission³⁰). The features of apoptosis vanished after removal of the cell death inducer (R24), indicating recovery of the cells (Figure 1A and B). Three biological replicates were performed at each time point. The principal component analysis indicated that all three biological replicates of each time point exhibited a very high correlation, as indicated by clustering, for the dataset of all 18 samples (Figure 2A; Supplementary Figure 1; see Data availability). The unsupervised hierarchical clustering confirms the similarity between all the replicates at each time point (Figure 2B; see Data availability; Supplementary Figure 2).

Genes that display significant changes in expression during anastasis at the earliest time point of 3 hours, following the removal of the cell death inducer, may represent critical first responders of anastasis (Figure 3A, Table 1), including transcription factors of the activator protein-1 (AP-1) family (Atf3, Fos, Fosb, Jun, Junb), transforming growth factor-β (TGF-β) signal pathway and its related regulators (Inhba, Snail, Tgfr1, Sox4, Sox9, Klf4, Klf6, Klf9), pro-survival Bcl-2 family member (Bag3),

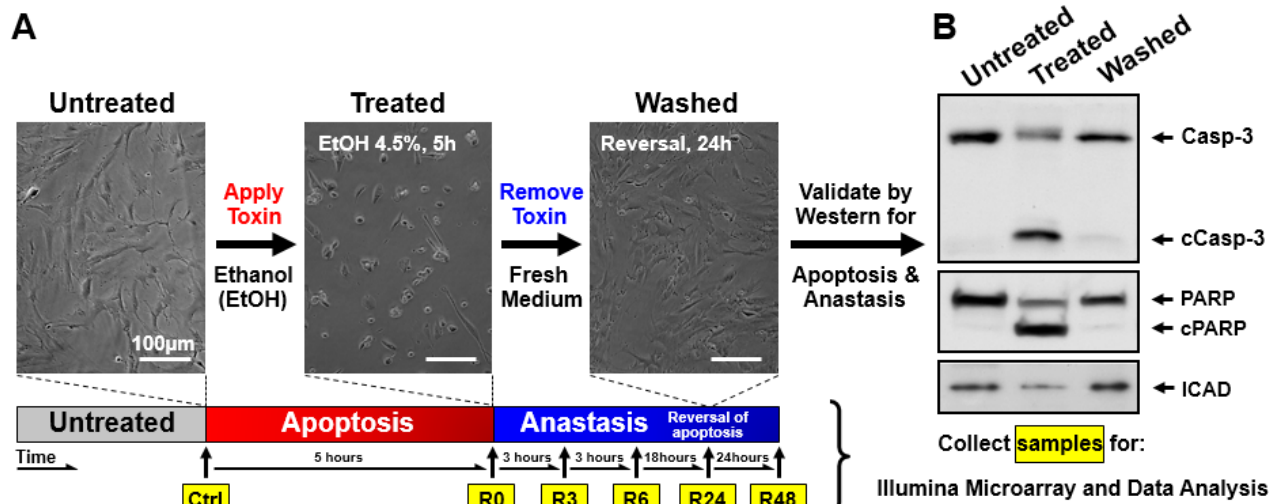


Figure 1. Flow chart for experimental design. Mouse primary liver cells were treated with 4.5% ethanol for 5 hours (R0) and then washed and cultured in fresh medium for 3 (R3), 6 (R6), 24 (R24), and 48 (R48) hours. The untreated cells served as control (Ctrl). (A) Time-lapse live-cell light microscopy and (B) Western blot analysis validated apoptosis to occur at R0, and anastasis at R24. Cells were collected at the indicated timepoints of (A) for RNA extraction. Gene expression profiling was performed by microarray, and analysed by Spotfire. The images from Figure 1A and B are adopted from the *Mol Biol Cell* 23, 2240–52 (2012)³⁰. Reprinted with permission.

inhibitor of p53 (Mdm2), anti-oxidation (Hmox1), anti-proliferation (Btg1), DNA damage (Ddit3, Ddit4), vesicular trafficking (Vps37b) and stress-inducible (Dnajb1, Dnajb9, Herpud1, Hspb1, Hspa1b) responses. Starting at 6 hours of anastasis, other groups of gene pathways display the peak of transcription, such as cell cycle arrest (Cdkn1a, Trp53inp1), autophagy (Atg12, Sqstm1), and cell migration (Mmp9, Mmp10 and Mmp13) (Figure 3B, Table 1 and Table 2). Expression of potent angiogenic factors, such as Vegfa and Angptl4, are up-regulated at 3 and 6 hours of anastasis, respectively (Table 1 and Table 2). Histones display up- (Hist1h2ae, H2afj) and down- (Hist1h2ak, Hist1h2ag, Hist1h2ap, Hist1h2af, Hist2h2ac, Hist1h2ah) regulations during the first 6 hours of anastasis (Table 2 and Table 3). Changes in expression of most of these genes peak at the 3–6-hour time points after removal of the apoptotic stimulus and then return to baseline (Figure 3A and B; Supplementary Figure 2). Interestingly, certain genes such as splicing of pre-mRNA (Rnu6), and growth arrest and DNA repair (Gadd45g) stay up-regulated during both apoptosis and anastasis (Figure 3C, Table 4).

We further observed the similar changes in gene expressions during anastasis in cultured human liver cancer HepG2 cells (Figure 4; see Data availability). The untreated HepG2 cells displayed tubular and filamentous mitochondria in the cells that spread on the substrate (Figure 4Ai, 4B). After exposure to 4.5% ethanol for 5 hours, the treated cells displayed morphological hallmarks of apoptosis, such as mitochondrial fragmentation, nuclear condensation, plasma membrane blebbing, and cell shrinkage (Figure 4Aii, 4B). After washed and incubated with fresh culture medium, the treated cells regained normal morphology (Figure 4Aiii, 4B). Interestingly, the HepG2 cells that underwent anastasis displayed the increase in micronuclei formation (Figure 4B), which is the biomarker of DNA damage⁵⁸, as we previously observed in mouse primary

liver cells, mouse embryonic fibroblast NIH 3T3 cells, human cervical cancer HeLa cells, and human small cell lung carcinoma H446 cells^{30,31}. By using reverse transcription polymerase chain reaction (RT-PCR), we verified our microarray data on HepG2 cells during reversal of ethanol-induced apoptosis, and found similar gene expression patterns during anastasis, including changes in mRNA levels of ANGPTL4, ATF3, ATG12, CDKN1A, FOS, HSPA1B, JUN, MDM2, MMP10 and SOX9 (Figure 4C; Supplementary Figure 3). This suggests that the mechanism of anastasis is conserved between primary and cancer cells.

The change in transcriptional profiles during anastasis provides us mechanistic insights into how dying cells could reverse apoptosis (Figure 5). In early anastasis, our data reveals that the regulators of the TGF- β signalling pathway, which control various fundamental cellular and pathological process, including proliferation, cell survival, apoptosis, cell migration, and transformation^{59–62}, are upregulated. The activation of the TGF- β pathway is further supported by the upregulation of AP-1 (Jun-Fos)⁵⁹, as observed here during early anastasis. The up-regulation of the TGF- β pathway can also promote the expression of murine double minute 2 (Mdm2)^{63,64}, an inhibitor of p53 that is also up-regulated during early anastasis³⁰. As p53 plays a critical role in regulating apoptosis and DNA repair^{65,66}, the expression of Mdm2 could not only promote cell survival by inhibiting p53-mediated cell death, but also cause mutations as we have observed in the cells after anastasis³⁰. Expression of Mdm2 can also activate XIAP⁶⁷, which inhibits caspases 3, 7 and 9^{68–73}, and therefore, could promote anastasis by suppressing the caspase-mediated cell destruction process. Up-regulation of anti-apoptotic BCL2 protein (Bag3) and heat shock proteins (Hsps) during anastasis can also neutralize pro-apoptotic proteins to promote cell recovery^{26,74,75}. Expression of Hmox1, which encodes heme oxygenase⁷⁶,

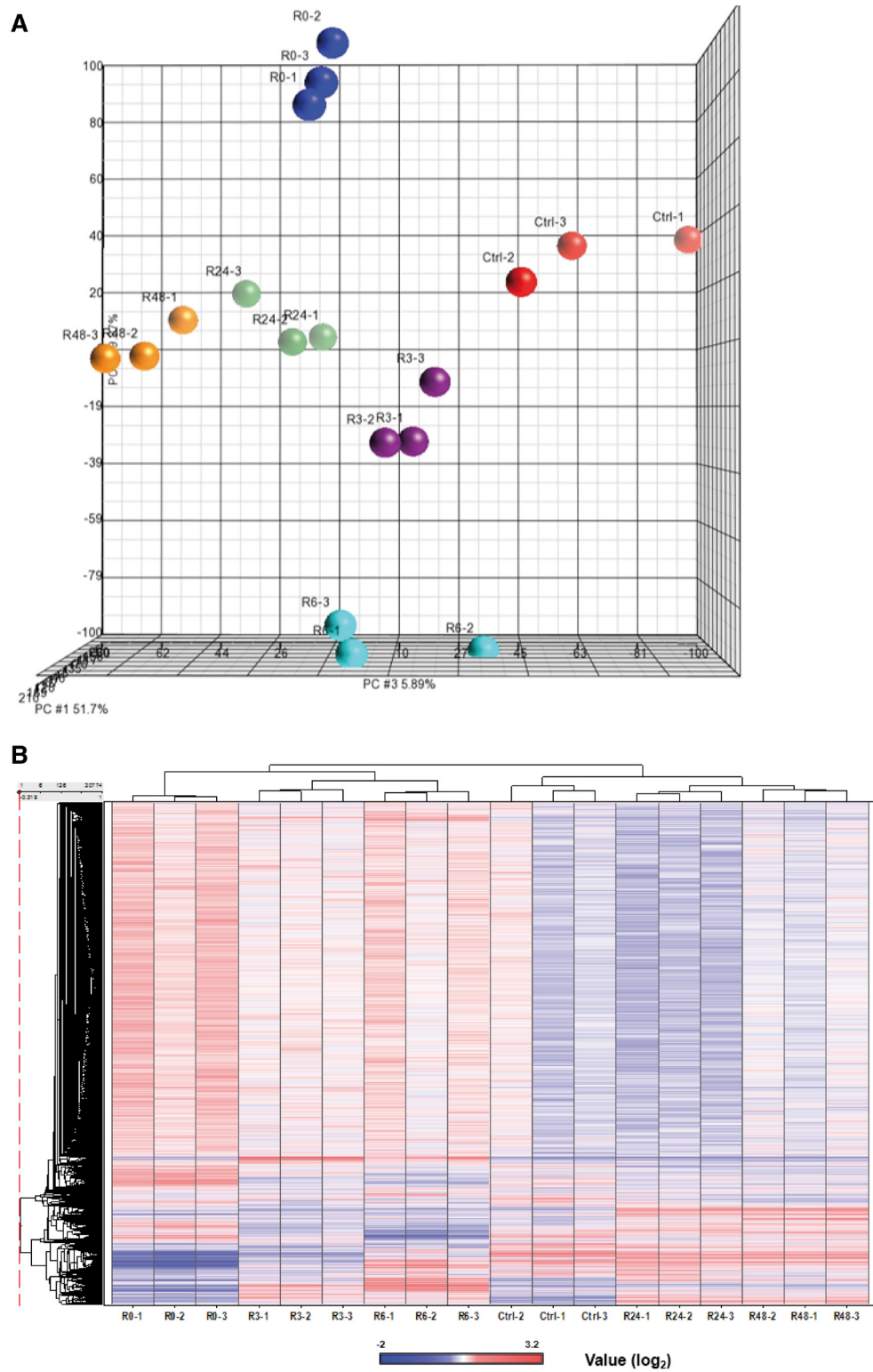


Figure 2. Technical validation of microarray data. The three biological replicate samples of microarray data were shown to cluster together by using **(A)** principal component analysis (PCA) and **(B)** unsupervised hierarchical clustering of the RNA microarray data of eighteen samples.

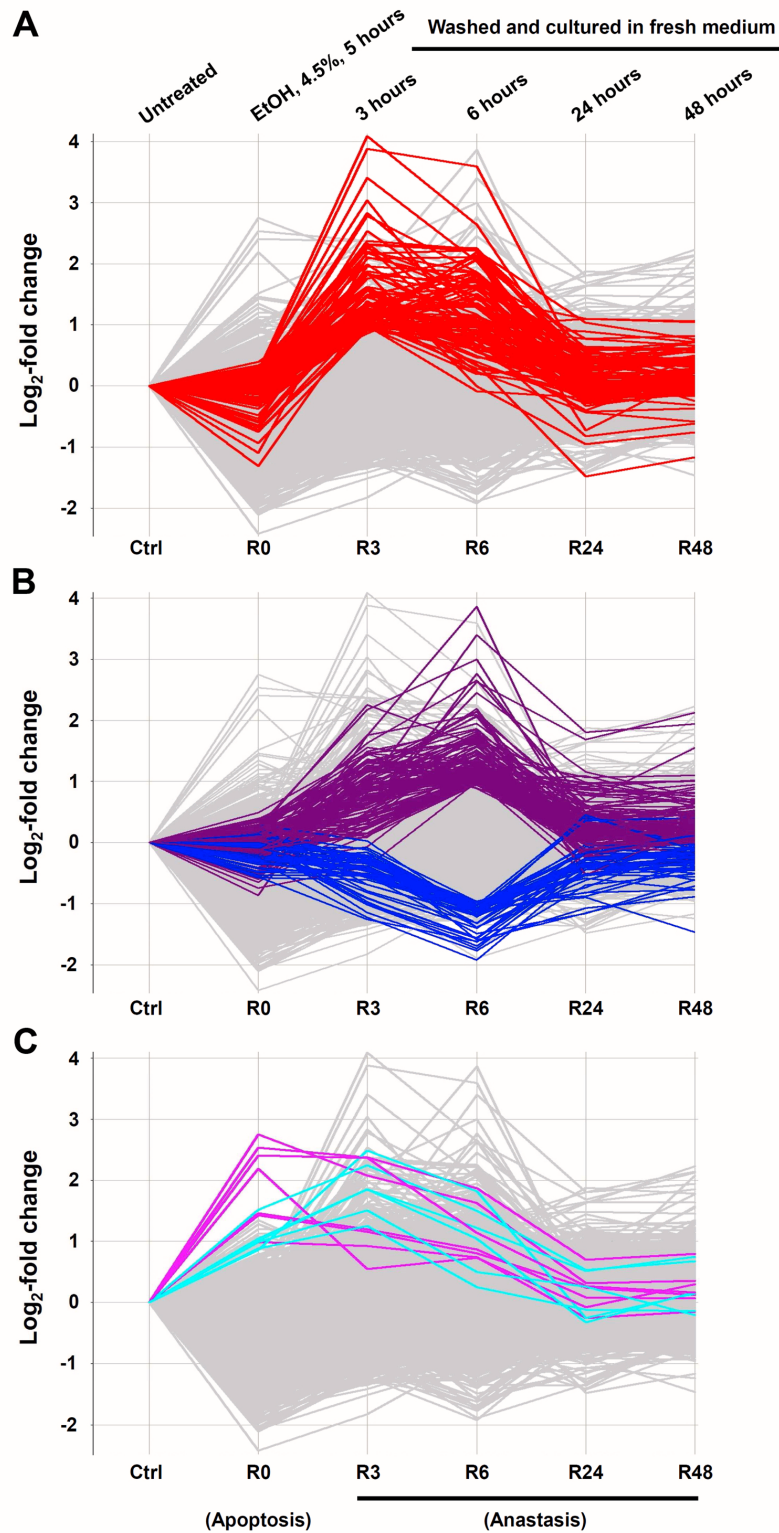


Figure 3. Change of gene expression profiles during reversal of apoptosis in mouse primary liver cells. Log₂-fold change of gene expression comparison between untreated cells (Ctrl), ethanol-induced apoptotic cells (R0), and induced cells that were then washed and further cultured in fresh medium for 3 (R3), 6 (R6), 24 (R24), and 48 (R48) hours. Genes that displayed specific **(A)** up-regulation at R3, **(B)** up- or down-regulation at R6, and **(C)** up-regulation anytime during the period from R0 to R6 with absolute log₂ fold change >1 are highlighted. The log₂ signal values from three biological replicates were averaged (geometric mean) for each time point.

Table 1. List of top 67 up-regulated genes at 3rd hour (R3) of anastasis, with log₂ fold change >1, compared with Ctrl (untreated cells).

Sort Order	Gene Symbol	Definition	Accession	Log ₂ fold change R3 vs. Ctrl
1	Atf3	activating transcription factor 3	NM_007498.2	4.08867
2	Hspa1b	heat shock protein 1B	NM_010478.2	3.88264
3	Fosb	FBJ osteosarcoma oncogene B	NM_008036.2	3.40725
4	Fos	FBJ osteosarcoma oncogene	NM_010234.2	3.03649
5	Egr2	no definition	NM_010118.1	2.82862
6	Dnajb1	DnaJ (Hsp40) homolog, subfamily B, member 1	NM_018808.1	2.78017
7	Dusp1	dual specificity phosphatase 1	NM_013642.2	2.533
8	Sox9	SRY-box containing gene 9	NM_011448.2	2.37421
9	Zfp36	zinc finger protein 36	NM_011756.4	2.33651
10	Mfsd11	no definition	AK007898	2.31434
11	Hspb1	no definition	NM_013560	2.30989
12	Jun	Jun oncogene	NM_010591.1	2.28214
13	Ddit4	DNA-damage-inducible transcript 4	NM_029083.1	2.25327
14	Vegfa	vascular endothelial growth factor A (Vegfa), transcript variant 1	NM_001025250.2	2.19637
15	Herpud1	homocysteine-inducible, ER stress-inducible, ubiquitin-like domain member 1	NM_022331.1	2.17913
16	Ddit3	DNA-damage inducible transcript 3	NM_007837.2	2.16334
17	Mdm2	transformed mouse 3T3 cell double minute 2	NM_010786.3	2.11273
18	Chac1	ChaC, cation transport regulator-like 1	NM_026929.3	2.08317
19	Arc	activity regulated cytoskeletal-associated protein	NM_018790.2	1.99046
20	Dnajb9	DnaJ (Hsp40) homolog, subfamily B, member 9	NM_013760.4	1.961
21	Zfand2a	zinc finger, AN1-type domain 2A	NM_133349.2	1.8778
22	Hes1	hairy and enhancer of split 1	NM_008235.2	1.85536
23	Bag3	BCL2-associated athanogene 3	NM_013863.4	1.85303
24	LOC100048331	PREDICTED: similar to DnaJ (Hsp40) homolog, subfamily A, member 4	XR_034509.1	1.82115
25	Hmox1	heme oxygenase	NM_010442.1	1.82111
26	Hspa5	heat shock protein 5	NM_022310.2	1.8205
27	Dlx2	distal-less homeobox 2	NM_010054.1	1.62035
28	6430590I03Rik	no definition	XM_489535	1.61804
29	Junb	Jun-B oncogene (Junb)	NM_008416.1	1.61245
30	LOC381140	no definition	XM_355056.1	1.57312
31	5430411C19Rik	PREDICTED: RIKEN cDNA 5430411C19 gene	XM_001478639.1	1.56805
32	Hspa1a	no definition	NM_010479	1.56028
33	Csrnp1	AXIN1 up-regulated 1	NM_153287.3	1.46632

Sort Order	Gene Symbol	Definition	Accession	Log ₂ fold change R3 vs. Ctrl
34	Tnfaip3	tumor necrosis factor, alpha-induced protein 3	NM_009397.2	1.45772
35	LOC100048105	PREDICTED: similar to Ubc protein, transcript variant 1	XM_001479832.1	1.45617
36	Bhlhe40	basic helix-loop-helix domain containing, class B2	NM_011498.4	1.39137
37	Dyrk3	dual-specificity tyrosine-(Y)-phosphorylation regulated kinase 3	NM_145508.2	1.3612
38	Egr1	early growth response 1	NM_007913.5	1.35873
39	Klf9	PREDICTED: RIKEN cDNA 2310051E17 gene	XM_001479552.1	1.35306
40	Snai1	snail homolog 1	NM_011427.2	1.35105
41	Dusp2	dual specificity phosphatase 2	NM_010090.2	1.34955
42	Ubg	no definition	no accession	1.3258
43	BC022687	cDNA sequence BC022687	NM_145450.3	1.31366
44	Btg1	B-cell translocation gene 1, anti-proliferative	NM_007569.1	1.2996
45	LOC100046232	PREDICTED: similar to NFIL3/E4BP4 transcription factor	XM_001475817.1	1.27509
46	Hsph1	no definition	NM_013559.1	1.2662
47	Hist1h2ae	histone cluster 1, H2ae	NM_178187.3	1.26359
48	mtDNA_ND4L	no definition	no accession	1.2474
49	Dnajb4	DnaJ (Hsp40) homolog, subfamily B, member 4	NM_025926.1	1.24227
50	Klf4	Kruppel-like factor 4	NM_010637.1	1.23324
51	Tgif1	TGFB-induced factor homeobox 1	NM_009372.2	1.22645
52	Klf6	Kruppel-like factor 6	NM_011803.2	1.22027
53	Ppp1r10	protein phosphatase 1, regulatory subunit 10	NM_175934.2	1.21047
54	Gm16516	no definition	NM_025293.1	1.20916
55	Ifrd1	interferon-related developmental regulator 1	NM_013562.1	1.19232
56	Slc23a3	solute carrier family 23 (nucleobase transporters), member 3	NM_194333.3	1.18765
57	Mfsd11	major facilitator superfamily domain containing 11	NM_178620.3	1.16606
58	Gm4589	PREDICTED: hypothetical protein LOC100045678	XM_001475512.1	1.16498
59	Klf9	Kruppel-like factor 9	NM_010638.4	1.12553
60	Siah2	seven in absentia 2	NM_009174.3	1.11181
61	Map1lc3b	microtubule-associated protein 1 light chain 3 beta	NM_026160.3	1.10454
62	Plk2	polo-like kinase 2	NM_152804.1	1.05963
63	Fgf21	fibroblast growth factor 21	NM_020013.4	1.05538
64	Id4	inhibitor of DNA binding 4	NM_031166.2	1.04488
65	Csf1	colony stimulating factor 1	NM_007778.3	1.03533
66	Bbc3	BCL2 binding component 3 (Bbc3)	NM_133234.1	1.03288
67	6230400G14Rik	no definition	no accession	1.02327

Table 2. List of top 109 up-regulated genes at 6th hour (R6) of anastasis, with log₂ fold change >0.93, compared with Ctrl (untreated cells).

Sort Order	Gene Symbol	Definition	Accession	Log ₂ fold change R6 vs. Ctrl
1	Inhba	inhibin beta-A	NM_008380.1	3.86584
2	Mmp10	matrix metalloproteinase 10	NM_019471.2	3.39644
3	Lce1f	late cornified envelope 1F	NM_026394.2	2.99957
4	Serpib2	serine (or cysteine) peptidase inhibitor, clade B, member 2	NM_011111.3	2.77022
5	Serpina3h	serine (or cysteine) peptidase inhibitor, clade A, member 3H	NM_001034870.2	2.65107
6	Mmp13	matrix metalloproteinase 13	NM_008607.1	2.62637
7	Ptpn22	protein tyrosine phosphatase, non-receptor type 22	NM_008979.1	2.45292
8	Rgs16	regulator of G-protein signaling 16	NM_011267.2	2.18647
9	Nppb	natriuretic peptide precursor type B	NM_008726.3	2.15071
10	Has1	hyaluronan synthase 1	NM_008215.1	2.14235
11	Dusp5	no definition	XM_140740.3	2.09536
12	Sqstm1	sequestosome 1	NM_011018.2	2.07477
13	Nupr1	nuclear protein 1	NM_019738.1	2.06313
14	Sphk1	sphingosine kinase 1 (Sphk1), transcript variant 2	NM_025367.5	1.94856
15	Dusp4	dual specificity phosphatase 4	NM_176933.4	1.85742
16	Klhl21	kelch-like 21	NM_001033352.3	1.84531
17	Lor	loricrin	NM_008508.2	1.81763
18	Ndrp1	N-myc downstream regulated gene 1	NM_008681.2	1.79158
19	Srxn1	sulfiredoxin 1 homolog	NM_029688.4	1.78335
20	Hk2	PREDICTED: hypothetical protein LOC100047934	XM_001478074.1	1.7519
21	Txnrd1	thioredoxin reductase 1 (Txnrd1), transcript variant 1	NM_001042523.1	1.75148
22	Angpt4	no definition	NM_020581	1.72982
23	Trib3	tribbles homolog 3	NM_175093.2	1.72246
24	C330006P03Rik	no definition	no accession	1.71297
25	Cdkn1a	cyclin-dependent kinase inhibitor 1A	NM_007669.2	1.69118
26	Gdf15	growth differentiation factor 15	NM_011819.1	1.67887
27	Prkg2	protein kinase, cGMP-dependent, type II	NM_008926.3	1.67374
28	H2afj	H2A histone family, member J	NM_177688.2	1.64825
29	Hbegf	heparin-binding EGF-like growth factor	NM_010415.1	1.61893
30	Trp53inp1	transformation related protein 53 inducible nuclear protein 1	NM_021897.1	1.61348
31	Gfpt2	glutamine fructose-6-phosphate transaminase 2	NM_013529.2	1.58159
32	Slc7a11	no definition	AK037490	1.57761
33	Ndrp1	no definition	NM_008681	1.5652
34	Gprc5a	G protein-coupled receptor, family C, group 5, member A	NM_181444.3	1.51339
35	Ibrdc3	no definition	XM_204030	1.49816
36	Ngf	nerve growth factor, beta	NM_013609.1	1.48619
37	Lce1d	late cornified envelope 1D	NM_027137.2	1.44977

Sort Order	Gene Symbol	Definition	Accession	Log ₂ fold change R6 vs. Ctrl
38	Tpsab1	tryptase alpha/beta 1	NM_031187.2	1.44267
39	Htr2b	5-hydroxytryptamine (serotonin) receptor 2B	NM_008311.2	1.43265
40	Sox4	SRY-box containing gene 4	NM_009238.2	1.41763
41	Il1rl1	interleukin 1 receptor-like 1 (Il1rl1), transcript variant 1	NM_001025602.1	1.3994
42	Prr9	RIKEN cDNA A030004J04 gene (A030004J04Rik)	NM_175424.3	1.36416
43	Vgf	VGF nerve growth factor inducible	NM_001039385.1	1.35246
44	Errfi1	ERBB receptor feedback inhibitor 1	NM_133753.1	1.34582
45	Il6	interleukin 6	NM_031168.1	1.33283
46	Gprc5a	no definition	NM_181444	1.31955
47	Antrx2	anthrax toxin receptor 2	NM_133738.1	1.30719
48	Tgif1	TGFB-induced factor homeobox 1	NM_009372.2	1.29814
49	Krt8	keratin 8	NM_031170.2	1.28819
50	2300009A05Rik	PREDICTED: RIKEN cDNA 2300009A05 gene, transcript variant 3	XM_898537.2	1.26684
51	Dppa5a	developmental pluripotency associated 5	NM_025274.1	1.258
52	Mt2	metallothionein 2	NM_008630.2	1.2441
53	Plaur	plasminogen activator, urokinase receptor	NM_011113.3	1.22553
54	Thbd	thrombomodulin	NM_009378.2	1.22252
55	LOC100047353	PREDICTED: similar to myocardial vascular inhibition factor	XM_001477963.1	1.22053
56	Csf2	colony stimulating factor 2 (granulocyte-macrophage)	NM_009969.4	1.22019
57	Map2k1	mitogen-activated protein kinase kinase 1	NM_008927.3	1.21788
58	Dpp7	dipeptidylpeptidase 7	NM_031843.2	1.21624
59	LOC672274	PREDICTED: similar to Transcription factor SOX-4	XR_003788.1	1.21149
60	Bicap	bladder cancer associated protein homolog	NM_016916.3	1.21046
61	Zfc3h1	no definition	NM_001033261.2	1.20585
62	Dusp6	dual specificity phosphatase 6	NM_026268.1	1.20441
63	Areg	amphiregulin	NM_009704.3	1.19656
64	C630022N07Rik	no definition	no accession	1.19569
65	Denr	density-regulated protein	NM_026603.1	1.18464
66	Slc3a2	solute carrier family 3 (activators of dibasic and neutral amino acid transport), member 2	NM_008577.3	1.18244
67	Ern1	endoplasmic reticulum (ER) to nucleus signalling 1	NM_023913.2	1.15145
68	Dnmt3l	DNA (cytosine-5-)-methyltransferase 3-like (Dnmt3l), transcript variant 2	NM_001081695.1	1.13992
69	D130007C19Rik	no definition	AK051152	1.13724
70	LOC100046401	PREDICTED: similar to SDR2	XR_032583.1	1.1332
71	Sh3bp2	SH3-domain binding protein 2	NM_011893.2	1.11999
72	Tgoln1	trans-golgi network protein	NM_009443.3	1.11454
73	Gm12226	similar to oxidative stress responsive 1 (Rp23-297j14.5)	NM_001099322.1	1.11231
74	Stk40	no definition	NM_028800	1.11149
75	Marcksl1	MARCKS-like 1 (Marcksl1), mRNA.	NM_010807.3	1.09791
76	Ypel5	yippee-like 5 (Drosophila) (Ypel5), mRNA.	NM_027166.3	1.08882
77	Fam180a	No definition	NM_173375	1.08779

Sort Order	Gene Symbol	Definition	Accession	Log ₂ fold change R6 vs. Ctrl
78	Creb3l2	cAMP responsive element binding protein 3-like 2 (Creb3l2), mRNA.	NM_178661.3	1.08689
79	Ly96	lymphocyte antigen 96 (Ly96), mRNA.	NM_016923.1	1.06285
80	Igf2bp2	insulin-like growth factor 2 mRNA binding protein 2 (Igf2bp2), mRNA.	NM_183029.1	1.06145
81	Mafg	v-maf musculoaponeurotic fibrosarcoma oncogene family, protein G	NM_010756.3	1.05594
82	Cttnbp2nl	No definition	NM_030249	1.04697
83	Col20a1	PREDICTED: collagen, type XX, alpha 1 (Col20a1), mRNA.	XM_181390.5	1.04143
84	Vps37b	vacuolar protein sorting 37B (yeast) (Vps37b), mRNA.	NM_177876.4	1.03812
85	A530046M15	No definition	XM_488663	1.03773
86	Eid3	EP300 interacting inhibitor of differentiation 3 (Eid3), mRNA.	NM_025499.2	1.03567
87	Nabp1	oligonucleotide/oligosaccharide-binding fold containing 2A (Obfc2a), mRNA.	NM_028696.2	1.0351
88	Pqlc1	PQ loop repeat containing 1 (Pqlc1), mRNA.	NM_025861.2	1.03363
89	Whrn	whirlin (Whrn), transcript variant 6, mRNA.	NM_001008795.1	1.0255
90	Cish	cytokine inducible SH2-containing protein (Cish), mRNA.	NM_009895.3	1.02328
91	Ptpre	protein tyrosine phosphatase, receptor type, E (Ptpre), mRNA.	NM_011212.2	1.01915
92	Bach1	BTB and CNC homology 1 (Bach1), mRNA.	NM_007520.2	1.01808
93	Cyb5r1	cytochrome b5 reductase 1 (Cyb5r1), mRNA.	NM_028057.2	1.01401
94	Slc1a4	solute carrier family 1 (glutamate/neutral amino acid transporter), member 4	NM_018861.2	1.00471
95	Mmd	no definition	AK033889	0.998067
96	Slc6a9	solute carrier family 6 (neurotransmitter transporter, glycine), member 9	NM_008135.4	0.994683
97	LOC100047963	PREDICTED: similar to ADIR1	XM_001479238.1	0.994667
98	Atf4	activating transcription factor 4	NM_009716.2	0.982833
99	Cttnbp2nl	CTTNBP2 N-terminal like	NM_030249.3	0.970113
100	Mmp9	matrix metalloproteinase 9	NM_013599.2	0.968853
101	Hmga1	high mobility group AT-hook 1	NM_016660.2	0.96846
102	Phlda1	pleckstrin homology-like domain, family A, member 1	NM_009344.1	0.963867
103	Aars	alanyl-tRNA synthetase	NM_146217.3	0.962397
104	Angpt2	angiopoietin 2	NM_007426.3	0.95926
105	Zswim4	zinc finger, SWIM domain containing 4	NM_172503.3	0.957373
106	Selk	no definition	NM_019979.1	0.954917
107	Abhd2	abhydrolase domain containing 2	NM_018811.6	0.954587
108	Krtap4-16	predicted gene, OTTMUSG00000002196	NM_001013823.1	0.95438
109	Atg12	autophagy-related 12	NM_026217.1	0.94998

Table 3. List of top 50 down-regulated genes at 6th hour (R6) of anastasis, with log₂ fold change <-0.95, compared with Ctrl (untreated cells).

Sort Order	Gene Symbol	Definition	Accession	Log ₂ fold change R6 vs. Ctrl
1	Hist1h2ak	histone cluster 1, H2ak	NM_178183.1	-1.91761
2	Hist1h2ag	histone cluster 1, H2ag	NM_178186.2	-1.76767
3	Hist1h2ap	histone cluster 1, H2ao	NM_178185.1	-1.7396
4	Hist1h2af	histone cluster 1, H2af	NM_175661.1	-1.6854
5	Hist2h2ac	histone cluster 2, H2ac	NM_175662.1	-1.6272
6	Slc1a3	solute carrier family 1 (glial high affinity glutamate transporter), member 3	NM_148938.2	-1.61827
7	9930013L23Rik	no definition	AK018112	-1.59264
8	Hist1h2ah	histone cluster 1, H2ah	NM_175659.1	-1.57002
9	Hist1h2al	PREDICTED: predicted gene, EG667728	XR_035278.1	-1.56907
10	Hist1h2ad	histone cluster 1, H2ad	NM_178188.3	-1.56233
11	Scel	sciellin	NM_022886.2	-1.48845
12	Hist1h2ai	histone cluster 1, H2ai	NM_178182.1	-1.40187
13	Fzd2	frizzled homolog 2	NM_020510.2	-1.38203
14	Sdpr	serum deprivation response	NM_138741.1	-1.38033
15	Hs3st1	heparan sulfate (glucosamine) 3-O-sulfotransferase 1	NM_010474.1	-1.32418
16	Hist2h2ab	histone cluster 2, H2ab	NM_178213.3	-1.30977
17	Kif2c	kinesin family member 2C (Kif2c) XM_986361	NM_134471.3	-1.21821
18	Fam198b	RIKEN cDNA 1110032E23 gene (1110032E23Rik)	NM_133187.2	-1.1988
19	Cdc42ep2	CDC42 effector protein (Rho GTPase binding) 2	NM_026772.1	-1.19681
20	Lurap1l	DNA segment, Chr 4, Brigham & Women's Genetics 0951 expressed (D4Bwg0951e)	NM_026821.4	-1.18656
21	Medag	RIKEN cDNA 6330406115 gene	NM_027519.1	-1.18243
22	Disp1	dispatched homolog 1	NM_026866.2	-1.18107
23	Bmp4	bone morphogenetic protein 4	NM_007554.2	-1.16637
24	Rab27a	RAB27A, member RAS oncogene family	NM_023635.4	-1.13917
25	Aurka	aurora kinase A	NM_011497.3	-1.12507
26	Ncaph	non-SMC condensin I complex, subunit H	NM_144818.1	-1.12132
27	Figl1	fidgetin-like 1	NM_021891.2	-1.10521
28	Dbp	D site albumin promoter binding protein	NM_016974.1	-1.09945
29	Meis2	Meis homeobox 2 (Meis2), transcript variant 2	NM_010825.2	-1.08487
30	Synpo	PREDICTED: synaptopodin, transcript variant 2	XM_981156.1	-1.08076
31	Hist1h2an	histone cluster 1, H2an	NM_178184.1	-1.0804
32	Fam111a	RIKEN cDNA 4632417K18 gene (4632417K18Rik)	NM_026640.2	-1.07617
33	Aurkb	aurora kinase B	NM_011496.1	-1.07507
34	Anln	anillin, actin binding protein	NM_028390.2	-1.07218
35	Tuft1	tuftelin 1	NM_011656.2	-1.06969
36	Cxcl12	chemokine (C-X-C motif) ligand 12 (Cxcl12), transcript variant 1	NM_021704.2	-1.0664
37	Sipa1l1	signal-induced proliferation-associated 1 like 1	NM_172579.1	-1.03567
38	Rbms2	RNA binding motif, single stranded interacting protein 2	NM_019711.2	-1.03096
39	Wdr6	WD repeat domain 6	NM_031392.2	-1.02705

Sort Order	Gene Symbol	Definition	Accession	Log ₂ fold change R6 vs. Ctrl
40	Tk1	thymidine kinase 1	NM_009387.1	-1.02669
41	Mylk	myosin, light polypeptide kinase	NM_139300.3	-1.01621
42	Slc9a3r1	solute carrier family 9 (sodium/hydrogen exchanger), member 3 regulator 1	NM_012030.2	-1.0137
43	Kif22	kinesin family member 22	NM_145588.1	-1.01346
44	Speer3	spermatogenesis associated glutamate (E)-rich protein 3	NM_027650.2	-1.01229
45	Mrgprf	MAS-related GPR, member F	NM_145379.2	-1.01038
46	Bub1b	budding uninhibited by benzimidazoles 1 homolog, beta	NM_009773.1	-1.00547
47	Pcgf5	polycomb group ring finger 5	NM_029508.3	-1.00513
48	Marcks	myristoylated alanine rich protein kinase C substrate	NM_008538.2	-0.973133
49	Fam83d	2310007D09Rik	NM_027975.1	-0.966323
50	Slc16a4	solute carrier family 16 (monocarboxylic acid transporters), member 4	NM_146136.1	-0.96461

Table 4. List of top 15 up-regulated genes during apoptosis (R0) and anastasis (R3 and R6), with log₂ fold change >1 either on R0, R3, or R6, compared with Ctrl (untreated cells).

Sort Order	Gene Symbol	Definition	Accession	Log ₂ fold change			
				R0 vs. Ctrl	R3 vs. Ctrl	R6 vs. Ctrl	R24 vs. Ctrl
1	Rnu6	U6 small nuclear RNA	NR_003027.1	2.75163	2.08117	1.63203	0.315967
2	Med23	no definition	AK042346	2.53792	2.37555	1.87041	0.70258
3	Prf1	perforin 1	NM_011073.2	2.40981	2.36444	1.1381	0.262567
4	F830002E14Rik	no definition	AK089567	2.18787	0.549207	0.731387	-0.08211
5	Slc11a1	solute carrier family 11 (proton-coupled divalent metal ion transporters), member 1	NM_013612.1	1.51837	2.24547	1.50337	0.53101
6	Hist1h4a	histone cluster 1, H4a	NM_178192.1	1.46352	1.19978	0.87087	0.08441
7	Hist1h4j	histone cluster 1, H4j	NM_178210.1	1.4276	1.15198	0.801933	0.241233
8	2310005L22Rik	no definition	no accession	1.19244	1.23574	0.79319	0.0878833
9	2810026P18Rik	no definition	no accession	1.12393	1.14743	0.527953	-0.31585
10	Gadd45g	growth arrest and DNA-damage-inducible 45 gamma	NM_011817.1	1.04177	1.85013	1.0444	-0.324567
11	Sppl3	no definition	AK047886	1.01269	1.85284	1.22205	0.51878
12	1810026B05Rik	no definition	XM_489186	0.9892	0.92441	0.742947	-0.257843
13	BC030476	cDNA sequence BC030476	NM_173421.1	0.98391	1.51116	0.495447	0.2612
14	Zbtb2	zinc finger and BTB domain containing 2	NM_001033466.1	0.882457	1.25171	0.253943	-0.116403
15	Ppp1r15a	myeloid differentiation primary response gene 116	NM_008654.1	0.862993	2.48696	1.82011	-0.25323

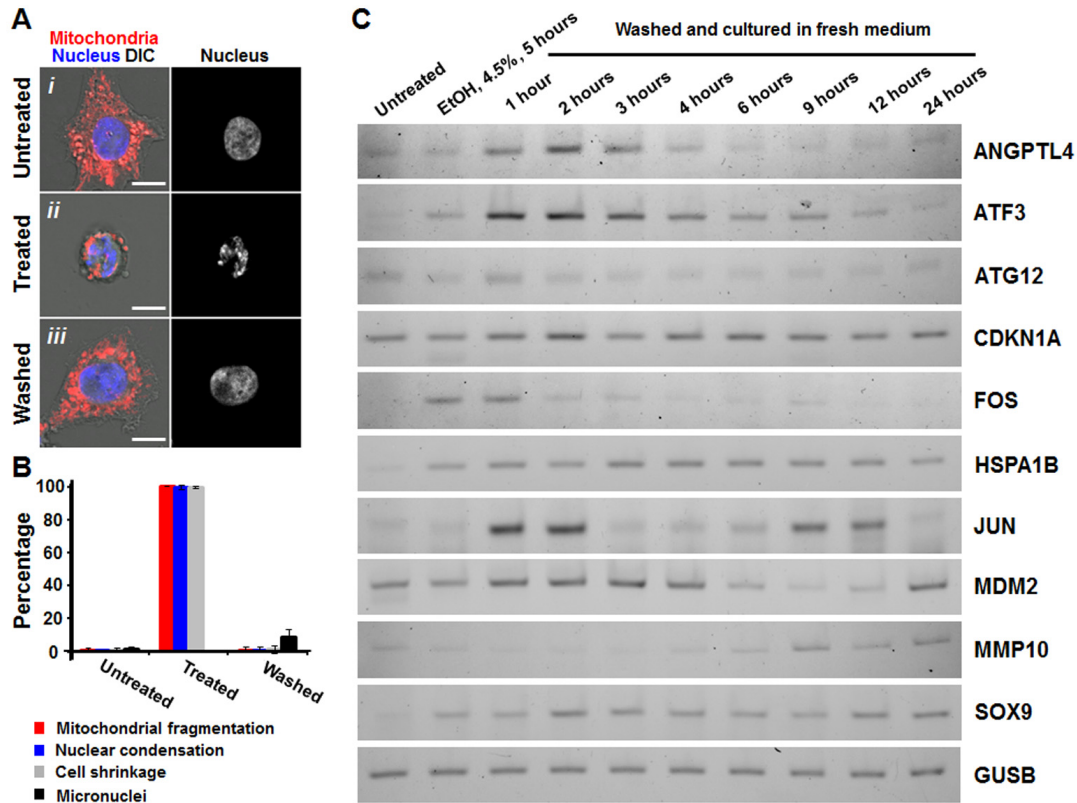


Figure 4. Change of gene expressions during reversal of apoptosis in human liver cancer HepG2 cells. (A) Confocal and differential interference contrast (DIC) microscopy of untreated liver cells (*i* Untreated), cells that were exposed to 4.5% ethanol for 5 hours (*ii* Treated), and the treated cells that were washed to remove apoptosis inducer and further cultured for 6 hours (*iii* Washed). Merged images, mitochondria (red) and nuclei (blue) were visualized by confocal microscopy and cell morphology by DIC. Monochrome images, nucleus of the corresponding cells. Scale bar, 10 μ m. (B) Quantification of the apoptotic response and its reversal on HepG2 cells. Percentage of the untreated cells, the treated cells (4.5% ethanol, 5 hours) and the washed cells (24 hours) showing mitochondrial fragmentation, nuclear condensation, cell shrinkage, and formation of micronuclei. (C) RT-PCR gel analysis of changes in mRNA levels of ANGPTL4, ATF3, ATG12, CDKN1A, FOS, GUSB, HSPA1B, JUN, MDM2, MMP10 and SOX9 on the untreated (Ctrl), the treated (R0, 4.5% ethanol for 5 hours), and the treated cells that were then washed and incubated in fresh medium for 1 hour (R1), 2 hours (R2), 3 hours (R3), 4 hours (R4), 6 hours (R6), 9 hours (R9), 12 hours (R12), and 24 hours (R24). GUSB serves as housekeeping gene. Sequences of primer sets for detecting targeted genes are available in Table 5.

Table 5. List of primer sequences for RT-PCR.

Gene	Accession number	Forward primer	Reverse primer	Amplicon
ANGPTL4	NM_139314.2	gacaagaactgcgccaaga	gccgttgagggtggaatg	72
ATF3	NM_001674.3	cgtgagtcctcgggtgctc	gcctgggtgtgaagcat	112
ATG12	NM_004707.3	tctccgctgcagttcc	gtctcccacagccttagca	87
CDKN1A	NM_000389.4	tgggtgtaccctctgga	tgaattcataaccgcctgtg	65
FOS	NM_005252	ctggcgttggaagaccat	ccttttctctctctctggagat	95
GUSB	NM_000181.3	cgccctgcctatctgtattc	tccccacaggagtggtgtag	91
HSPA1B	NM_005346.4	gggtcaggccctaccatt	caacagtccacctcaagacaa	77
JUN	NM_002228.3	ccaagagatagtcgatgttt	ctgtccctctcactgcaac	62
MDM2	NM_002392.5	tctgatagtattccccttctcttg	tggtcacttacaccagcatcaa	137
MMP10	NM_002425.2	gcattttggccctctcttc	cagggtatggatgcctcttg	147
SOX9	NM_000346.3	gtaccgcactgcacaac	tctcgctctcgttcagaagtc	74

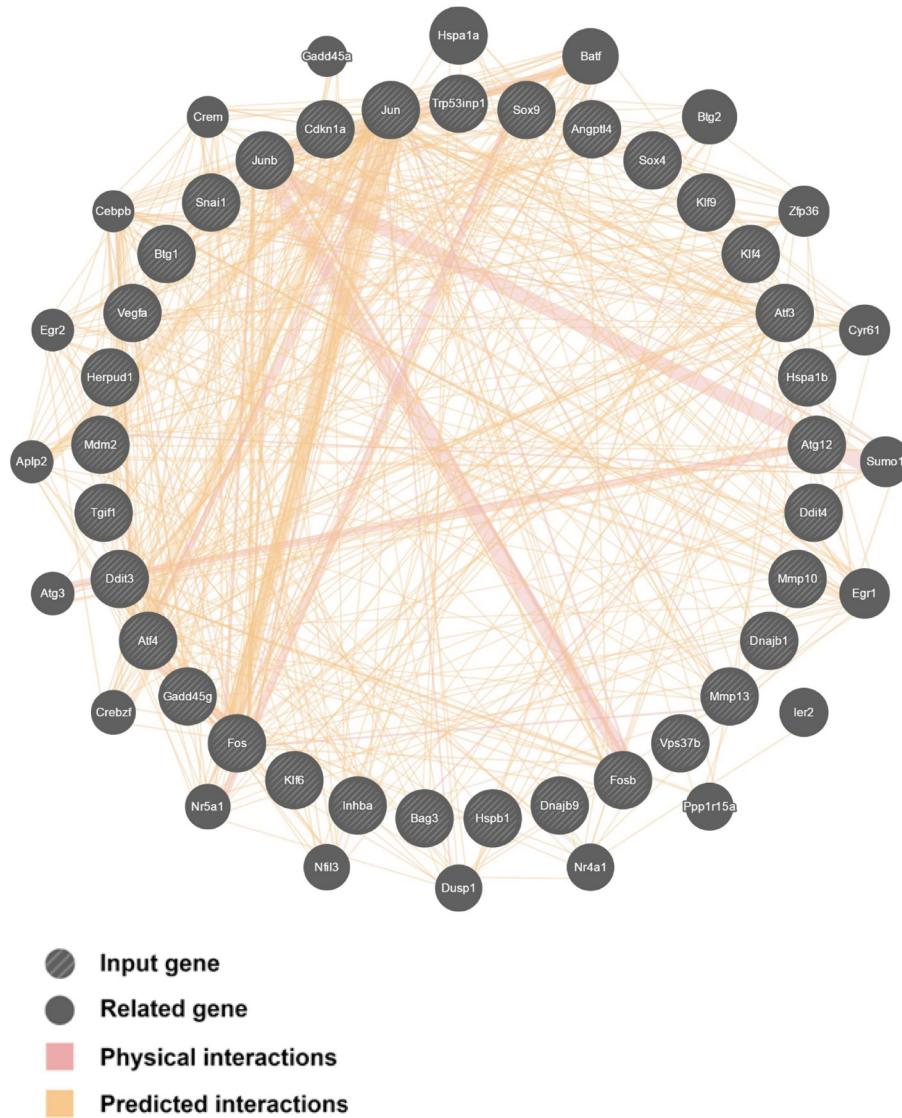


Figure 5. Interaction network of the up-regulated genes during anastasis. The 33 up-regulated genes during anastasis were selected for analysis using GeneMANIA.

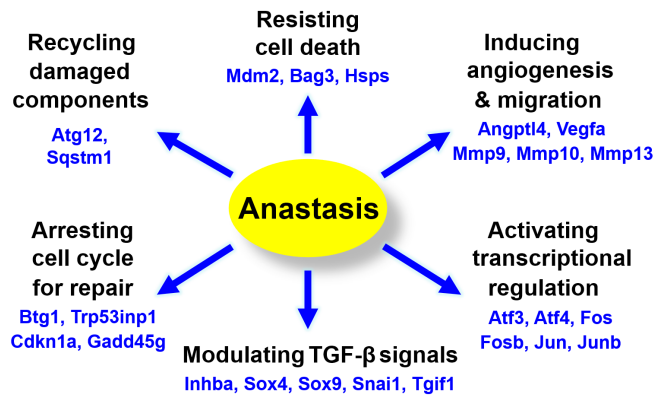


Figure 6. Up-regulation of genes and potential corresponding pathways during reversal of apoptosis.

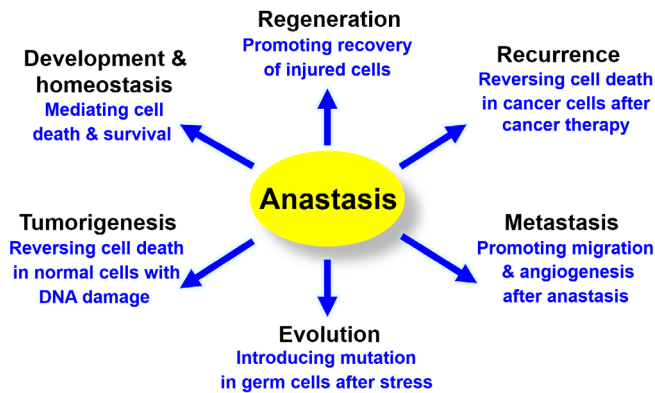


Figure 7. Potential consequences of anastasis.

could protect dying cells from free radicals that are generated during apoptosis. Notably, the expression of Bbc3, a pro-apoptotic BH3-only gene to encode PUMA (p53 upregulated modulator of apoptosis)^{77,78}, peaks at anastasis (R3-R6), suggesting the sign of anastasis vs apoptosis in the recovering cells during the early stage of the cell recovery process.

To reverse apoptosis, the recovering cells need to remove or recycle the destroyed cellular components, such as the toxic or damaged proteins that are cleaved by caspases, and dysfunctional organelles like the permeabilized mitochondria. Autophagy could contribute to anastasis, as the recovering cells display up-regulation of Atg12 (Figure 3B, Table 2), which is important to the formation of autophagosome to engulf the materials that are then transported to lysosomes or vacuoles for degradation⁷⁹⁻⁸². Sqstm1, which encodes sequestosome 1⁸³⁻⁸⁵ and is up-regulated at R6, could play important role in mediating autophagy and DNA damage response during anastasis. In fact, recently studies reveal that autophagy can be activated by the DNA damage response, and play a role in maintaining the nuclear and mitochondrial genomic integrity through DNA repair and removal of micronuclei and damaged nuclear parts^{86,87}. This could suppress mutagenesis and oncogenic transformation to occur in the cells that reverse apoptosis as we have observed after DNA damage^{30,31}. Autophagy is also implicated in the exosome secretory pathway⁸⁸⁻⁹⁰, which could allow rapid clearance of damaged or toxic materials during anastasis through exosomes. Interestingly, our microarray data shows that the recovering cells display up-regulation of potent angiogenic factors such as Vegfa and Angptl4 (Figure 3A and B, Table 1 and Table 2), which promote vascular permeability and angiogenesis⁹¹⁻⁹⁴. This could facilitate anastasis by supplying nutrient and clearing waste products. However, this could also enhance tumour recurrence, progression and metastasis⁹⁵, when anastasis occurs in cancer cells between cycles of cancer therapy. In fact, our data also reveals the up-regulation of genes involved in cell migration during anastasis³⁰, such as Mmp 9, 10 and 13 (Figure 3B, Table 2) that encode matrix metalloproteinases⁹⁶⁻⁹⁹. This could be a stress-inducible response that promotes cell migration, like what we have observed in HeLa cells after anastasis (Supplementary

Figure 4)³¹, which might contribute to wound healing after tissue injury, or metastasis during cancer recurrence^{100,101}.

Change in expression of histone proteins contributes to histone modification, which plays critical role in transcription, DNA replication and repairing¹⁰²⁻¹⁰⁶. At the late stage of anastasis (R6), various histone genes display significant changes in expression (Table 2, Table 3), suggesting potential connection between histone modification and reversal of apoptosis. Interestingly, significant number of histone genes are down-regulated during anastasis (Table 3). Recent study reported histone degradation in response to DNA damage, and that is important for DNA repairing¹⁰⁷. As dying cells can reverse apoptosis after DNA damage^{30,31}, reduction of histone gene expression could represent the DNA damage response during anastasis.

Arresting cell cycle during anastasis is important as it can allow damaged cells to be repaired before they restore proliferation. This hypothesis is supported by our microarray data that reveals up-regulation of genes that suppress cell cycle (Figure 3A-C). For example, B-cell translocation gene 1 (Btg1) is an anti-proliferative gene^{108,109}, which is up-regulated during the early anastasis (R3). At later stage of anastasis (R6), other cell cycle inhibitors express, including Cdkn1a which encodes p21 that induces cell cycle arrest and senescence¹¹⁰⁻¹¹², and also Trp53inp1 which encodes tumor protein p53-inducible nuclear protein 1 that can arrest cell cycle independent to p53 expression¹¹³. These suggest that cell cycle is suppressed by multiple pathways during anastasis.

We also identified genes that are up-regulated both during apoptosis and anastasis, such as Gadd45g, and Rnu6 (Figure 3C, Table 4). Gadd45g functions in growth arrest and DNA repair^{114,115}, and therefore, could be the cytoprotective mechanism that preserves DNA in the dying cells during cell death induction (R0), and promotes the injured cells to repair when the environment is improved (R3 and R6). Rnu6 encodes U6 small nuclear RNA, which is important for splicing of a mammalian pre-mRNA¹¹⁶⁻¹¹⁹. Upregulation of Rnu6 from R0 to R6 suggests that post-transcriptional regulation could be involved during apoptosis and anastasis. In fact, translational regulation also contributes to anastasis. For example, caspase-3, PARP and ICAD are cleaved in dying cells during apoptosis, and the non-cleaved form of corresponding proteins restores after anastasis (Figure 1B). Interestingly, the mRNA level of caspase-3, PARP and ICAD did not show significant increase during and after anastasis (see Data availability). This suggests the contribution of translational regulation during anastasis.

Our study provides new insights into the mechanisms and consequences of anastasis (Figure 6). Researchers can analyse our microarray data to further identify the hallmarks of anastasis, understand its role, elucidate molecular mechanisms that reverse apoptosis, and develop therapeutic strategies by controlling anastasis. To identify the genes that display specific change on a transcriptional level, software such as Spotfire can be used to view the gene expression pattern at different time points during the reversal of

apoptosis⁵⁴. To study the molecular mechanism of anastasis, Ingenuity Pathway Analysis can be used to create mechanistic hypotheses according to the transcriptional profile¹²⁰. To identify drugs that modulate anastasis, Connectivity Map can be used to identify small molecules that promote or suppress anastasis based on its gene expression signature^{121,122}. Anastasis could be a cell survival phenomenon mediated by multiple pathways^{29–31,33}, so by comparing the gene expression profiles, researchers can study its potential connection to other cellular processes, such as anti-apoptotic pathways, autophagy, and stress-inducible responses^{82,123–127}. By searching the molecular signature of anastasis, researchers can study its potential contribution to physiological and pathological conditions, such as recovery from heart failure, wound healing, mutagenesis, tumour evolution, cancer recurrence and metastasis^{45,100,101,128}. Further data analysis will stimulate the generation of hypotheses for future studies involving anastasis. As our understanding of anastasis mechanism expands, it will uncover its potential impacts on physiology and pathology, and offer exciting new therapeutic opportunities to intractable diseases by mediating cell death and survival (Figure 7).

Data availability

Figshare: Raw data for Tang *et al.*, 2016 “Molecular signature of anastasis for reversal of apoptosis” doi: [10.6084/m9.figshare.4502732](https://doi.org/10.6084/m9.figshare.4502732)

<http://dx.doi.org/10.6084/m9.figshare.4502732>

Author contributions

H.L.T., H.M.T. and M.C.F. conceived the idea and designed the research; H.L.T. and H.M.T. wrote the article, conducted the analyses together with C.C.T. and M.C.F. All authors agreed to the final content of the manuscript.

Competing interests

No competing interests were disclosed.

Grant information

This work was supported by the Shurl and Kay Curci Foundation of the Life Sciences Research Foundation fellowship (H.L.T.).

The funders had no role in study design, data collection and analysis, decision to publish, or preparation of the manuscript.

Acknowledgments

We thank J. Marie Hardwick for valuable advice to this work, and the Johns Hopkins Deep Sequencing and Microarray Core Facility for data analysis. Ho Lam Tang is a Shurl and Kay Curci Foundation Fellow of the Life Sciences Research Foundation.

Supplementary material

Supplementary Figure 1: Technical validation of microarray data. The three biological replicate samples of microarray data were shown to cluster together by using principal component analysis (PCA).

Supplementary Figure 2: Genes display unique expression patterns at each timepoint. Output of all genes analysed by Spotfire (K cluster, also see Data availability).

Supplementary Figure 3: Uncropped agarose gel images. RT-PCR gel analysis of changes in mRNA levels of ANGPTL4, ATF3, ATG12, CDKN1A, FOS, HSPA1B, JUN, MDM2, MMP10 and SOX9 on untreated (Lane 1: Ctrl), treated (Lane 2: R0, 4.5% ethanol for 5 hours), and the treated cells that were then washed and incubated in fresh medium for 1 hour (Lane 3: R1), 2 hours (Lane 4: R2), 3 hours (Lane 5: R3), 4 hours (Lane 6: R4), 6 hours (Lane 7: R6), 9 hours (Lane 8: R9), 12 hours (Lane 9: R12), and 24 hours (Lane 10: R24). GUSB serves as housekeeping gene. Lane M is loaded with 25 bp DNA Ladder (Invitrogen). Sequences of primer sets for detecting targeted genes are available in Table 5.

Supplementary Figure 4: Increase in mobility of HeLa cells after reversal of ethanol-induced apoptosis. Time-lapse live-cell fluorescence microscopy of HeLa cells before, during, and after exposure to the apoptotic stimulus, ethanol. The same cells before ethanol induction (Untreated, *i*), induced with 5% ethanol in culture medium for 55 minutes (Induced, *ii* to *iv*), and then washed and further cultured with fresh medium (Washed, *v* to *xx*). Green, white and yellow lines indicate the footprints of the corresponding same cells that reversed apoptosis throughout the experiment with time. Cells without displayed hallmarks of apoptosis at late stage, such as cell shrinkage and nucleus condensation (without track), had lower mobility than the tracked cells. Merged images, mitochondria (red) and nuclei (blue) were visualized by fluorescence, and cell morphology by differential interference contrast (DIC) microscopy. Time presented as hour:minute. Scale bar, 10 μ m. Adopted images reprinted with permission¹²⁹.

[Click here to access Supplementary Figures.](#)

References

1. Kerr JF, Wyllie AH, Currie AR: **Apoptosis: a basic biological phenomenon with wide-ranging implications in tissue kinetics.** *Br J Cancer.* 1972; **26**(4): 239–57.
[PubMed Abstract](#) | [Publisher Full Text](#) | [Free Full Text](#)
2. Jacobson MD, Weil M, Raff MC: **Programmed cell death in animal development.** *Cell.* 1997; **88**(3): 347–54.
[PubMed Abstract](#) | [Publisher Full Text](#)
3. Fuchs Y, Steller H: **Programmed cell death in animal development and disease.** *Cell.* 2011; **147**(4): 742–58.
[PubMed Abstract](#) | [Publisher Full Text](#) | [Free Full Text](#)
4. Riedl SJ, Shi Y: **Molecular mechanisms of caspase regulation during apoptosis.** *Nat Rev Mol Cell Biol.* 2004; **5**(11): 897–907.
[PubMed Abstract](#) | [Publisher Full Text](#)
5. Green DR, Kroemer G: **The pathophysiology of mitochondrial cell death.** *Science.* 2004; **305**(5684): 626–9.
[PubMed Abstract](#) | [Publisher Full Text](#)
6. Chipuk JE, Bouchier-Hayes L, Green DR: **Mitochondrial outer membrane permeabilization during apoptosis: the innocent bystander scenario.** *Cell Death Differ.* 2006; **13**(8): 1396–402.
[PubMed Abstract](#) | [Publisher Full Text](#)
7. Kroemer G, Galluzzi L, Vandenabeele P, *et al.*: **Classification of cell death: recommendations of the Nomenclature Committee on Cell Death 2009.** *Cell Death Differ.* 2009; **16**(1): 3–11.
[PubMed Abstract](#) | [Publisher Full Text](#) | [Free Full Text](#)
8. Galluzzi L, Vitale I, Abrams JM, *et al.*: **Molecular definitions of cell death subroutines: recommendations of the Nomenclature Committee on Cell Death 2012.** *Cell Death Differ.* 2012; **19**(1): 107–20.
[PubMed Abstract](#) | [Publisher Full Text](#) | [Free Full Text](#)
9. Holland AJ, Cleveland DW: **Chromosomal rearrangements and cancer: mechanisms and consequences of localized, complex chromosomal rearrangements.** *Nat Med.* 2012; **18**(11): 1630–8.
[PubMed Abstract](#) | [Publisher Full Text](#) | [Free Full Text](#)
10. Wang X: **The expanding role of mitochondria in apoptosis.** *Genes Dev.* 2001; **15**(22): 2922–33.
[PubMed Abstract](#)
11. Galluzzi L, Kepp O, Kroemer G: **Mitochondria: master regulators of danger signalling.** *Nat Rev Mol Cell Biol.* 2012; **13**(12): 780–8.
[PubMed Abstract](#) | [Publisher Full Text](#)
12. Du C, Fang M, Li Y, *et al.*: **Smac, a mitochondrial protein that promotes cytochrome c-dependent caspase activation by eliminating IAP inhibition.** *Cell.* 2000; **102**(1): 33–42.
[PubMed Abstract](#) | [Publisher Full Text](#)
13. Verhagen AM, Ekert PG, Pakusch M, *et al.*: **Identification of DIABLO, a mammalian protein that promotes apoptosis by binding to and antagonizing IAP proteins.** *Cell.* 2000; **102**(1): 43–53.
[PubMed Abstract](#) | [Publisher Full Text](#)
14. Susin SA, Lorenzo HK, Zamzami N, *et al.*: **Molecular characterization of mitochondrial apoptosis-inducing factor.** *Nature.* 1999; **397**(6718): 441–6.
[PubMed Abstract](#) | [Publisher Full Text](#)
15. Miramar MD, Costantini P, Ravagnan L, *et al.*: **NADH oxidase activity of mitochondrial apoptosis-inducing factor.** *J Biol Chem.* 2001; **276**(19): 16391–8.
[PubMed Abstract](#) | [Publisher Full Text](#)
16. Joza N, Susin SA, Daugas E, *et al.*: **Essential role of the mitochondrial apoptosis-inducing factor in programmed cell death.** *Nature.* 2001; **410**(6828): 549–54.
[PubMed Abstract](#) | [Publisher Full Text](#)
17. Li LY, Luo X, Wang X: **Endonuclease G is an apoptotic DNase when released from mitochondria.** *Nature.* 2001; **412**(6842): 95–9.
[PubMed Abstract](#) | [Publisher Full Text](#)
18. Lüthi AU, Martin SJ: **The CASBAH: a searchable database of caspase substrates.** *Cell Death Differ.* 2007; **14**(4): 641–50.
[PubMed Abstract](#) | [Publisher Full Text](#)
19. Liu X, Zou H, Slaughter C, *et al.*: **DFF, a heterodimeric protein that functions downstream of caspase-3 to trigger DNA fragmentation during apoptosis.** *Cell.* 1997; **89**(2): 175–84.
[PubMed Abstract](#) | [Publisher Full Text](#)
20. Enari M, Sakahira H, Yokoyama H, *et al.*: **A caspase-activated DNase that degrades DNA during apoptosis, and its inhibitor ICAD.** *Nature.* 1998; **391**(6662): 43–50.
[PubMed Abstract](#) | [Publisher Full Text](#)
21. Mukae N, Enari M, Sakahira H, *et al.*: **Molecular cloning and characterization of human caspase-activated DNase.** *Proc Natl Acad Sci U S A.* 1998; **95**(16): 9123–8.
[PubMed Abstract](#) | [Publisher Full Text](#) | [Free Full Text](#)
22. Coleman ML, Sahai EA, Yeo M, *et al.*: **Membrane blebbing during apoptosis results from caspase-mediated activation of ROCK I.** *Nat Cell Biol.* 2001; **3**(4): 339–45.
[PubMed Abstract](#) | [Publisher Full Text](#)
23. Orlando KA, Stone NL, Pittman RN: **Rho kinase regulates fragmentation and phagocytosis of apoptotic cells.** *Exp Cell Res.* 2006; **312**(1): 5–15.
[PubMed Abstract](#) | [Publisher Full Text](#)
24. Tyas L, Brophy VA, Pope A, *et al.*: **Rapid caspase-3 activation during apoptosis revealed using fluorescence-resonance energy transfer.** *EMBO Rep.* 2000; **1**(3): 266–70.
[PubMed Abstract](#) | [Publisher Full Text](#) | [Free Full Text](#)
25. Takemoto K, Nagai T, Miyawaki A, *et al.*: **Spatio-temporal activation of caspase revealed by indicator that is insensitive to environmental effects.** *J Cell Biol.* 2003; **160**(2): 235–43.
[PubMed Abstract](#) | [Publisher Full Text](#) | [Free Full Text](#)
26. Chipuk JE, Moldoveanu T, Lambi F, *et al.*: **The BCL-2 family reunion.** *Mol Cell.* 2010; **37**(3): 299–310.
[PubMed Abstract](#) | [Publisher Full Text](#) | [Free Full Text](#)
27. Hammill AK, Uhr JW, Scheuermann RH: **Annexin V staining due to loss of membrane asymmetry can be reversible and precede commitment to apoptotic death.** *Exp Cell Res.* 1999; **251**(1): 16–21.
[PubMed Abstract](#) | [Publisher Full Text](#)
28. Geske FJ, Lieberman R, Strange R, *et al.*: **Early stages of p53-induced apoptosis are reversible.** *Cell Death Differ.* 2001; **8**(2): 182–91.
[PubMed Abstract](#) | [Publisher Full Text](#)
29. Tang HL, Yuen KL, Tang HM, *et al.*: **Reversibility of apoptosis in cancer cells.** *Br J Cancer.* 2009; **100**(1): 118–22.
[PubMed Abstract](#) | [Publisher Full Text](#) | [Free Full Text](#)
30. Tang HL, Tang HM, Mak KH, *et al.*: **Cell survival, DNA damage, and oncogenic transformation after a transient and reversible apoptotic response.** *Mol Biol Cell.* 2012; **23**(12): 2240–52.
[PubMed Abstract](#) | [Publisher Full Text](#) | [Free Full Text](#)
31. Tang HL, Tang HM, Hardwick JM, *et al.*: **Strategies for tracking anastasis, a cell survival phenomenon that reverses apoptosis.** *J Vis Exp.* 2015; (96).
[PubMed Abstract](#) | [Publisher Full Text](#)
32. Ichim G, Lopez J, Ahmed SU, *et al.*: **Limited mitochondrial permeabilization causes DNA damage and genomic instability in the absence of cell death.** *Mol Cell.* 2015; **57**(5): 860–72.
[PubMed Abstract](#) | [Publisher Full Text](#) | [Free Full Text](#)
33. Tang HL, Tang HM, Fung MC, *et al.*: **In vivo CaspaseTracker biosensor system for detecting anastasis and non-apoptotic caspase activity.** *Sci Rep.* 2015; **5**: 9015.
[PubMed Abstract](#) | [Publisher Full Text](#) | [Free Full Text](#)
34. Ding AX, Sun G, Argaw YG, *et al.*: **CasExpress reveals widespread and diverse patterns of cell survival of caspase-3 activation during development in vivo.** *eLife.* 2016; **5**: pii: e10936.
[PubMed Abstract](#) | [Publisher Full Text](#) | [Free Full Text](#)
35. Taylor RC, Cullen SP, Martin SJ: **Apoptosis: controlled demolition at the cellular level.** *Nat Rev Mol Cell Biol.* 2008; **9**(3): 231–41.
[PubMed Abstract](#) | [Publisher Full Text](#)
36. Davis AJ, Tannock JF: **Repopulation of tumour cells between cycles of chemotherapy: a neglected factor.** *Lancet Oncol.* 2000; **1**(2): 86–93.
[PubMed Abstract](#) | [Publisher Full Text](#)
37. Kim JJ, Tannock IF: **Repopulation of cancer cells during therapy: an important cause of treatment failure.** *Nat Rev Cancer.* 2005; **5**(7): 516–25.
[PubMed Abstract](#) | [Publisher Full Text](#)
38. Wagle N, Emery C, Berger MF, *et al.*: **Dissecting therapeutic resistance to RAF inhibition in melanoma by tumor genomic profiling.** *J Clin Oncol.* 2011; **29**(22): 3085–96.
[PubMed Abstract](#) | [Publisher Full Text](#) | [Free Full Text](#)
39. Manjila S, Ray A, Hu Y, *et al.*: **Embryonal tumors with abundant neuropil and true rosettes: 2 illustrative cases and a review of the literature.** *Neurosurg Focus.* 2011; **30**(1): E2.
[PubMed Abstract](#) | [Publisher Full Text](#)
40. Boffetta P, Hashibe M: **Alcohol and cancer.** *Lancet Oncol.* 2006; **7**(2): 149–56.
[PubMed Abstract](#) | [Publisher Full Text](#)
41. McKillop IH, Schrum LW: **Alcohol and liver cancer.** *Alcohol.* 2005; **35**(3): 195–203.
[PubMed Abstract](#) | [Publisher Full Text](#)
42. Castellsagué X, Muñoz N, De Stefani E, *et al.*: **Influence of mate drinking, hot beverages and diet on esophageal cancer risk in South America.** *Int J Cancer.* 2000; **88**(4): 658–64.
[PubMed Abstract](#) | [Publisher Full Text](#)
43. Islami F, Pourshams A, Nasrollahzadeh D, *et al.*: **Tea drinking habits and oesophageal cancer in a high risk area in northern Iran: population based case-control study.** *BMJ.* 2009; **338**: b929.
[PubMed Abstract](#) | [Publisher Full Text](#) | [Free Full Text](#)
44. Loomis D, Guyton KZ, Grosse Y, *et al.*: **Carcinogenicity of drinking coffee, mate, and very hot beverages.** *Lancet Oncol.* 2016; **17**(7): 877–8.
[PubMed Abstract](#) | [Publisher Full Text](#)
45. Yates LR, Campbell PJ: **Evolution of the cancer genome.** *Nat Rev Genet.* 2012; **13**(11): 795–806.
[PubMed Abstract](#) | [Publisher Full Text](#) | [Free Full Text](#)
46. Smith RE, Bryant J, DeCillis A, *et al.*: **Acute myeloid leukemia and myelodysplastic**

- syndrome after doxorubicin-cyclophosphamide adjuvant therapy for operable breast cancer: the National Surgical Adjuvant Breast and Bowel Project Experience. *J Clin Oncol*. 2003; **21**(7): 1195–204.
[PubMed Abstract](#) | [Publisher Full Text](#)
47. Travis LB, Fossá SD, Schonfeld SJ, *et al.*: **Second cancers among 40,576 testicular cancer patients: focus on long-term survivors.** *J Natl Cancer Inst*. 2005; **97**(18): 1354–65.
[PubMed Abstract](#) | [Publisher Full Text](#)
48. Chaturvedi AK, Engels EA, Gilbert ES, *et al.*: **Second cancers among 104,760 survivors of cervical cancer: evaluation of long-term risk.** *J Natl Cancer Inst*. 2007; **99**(21): 1634–43.
[PubMed Abstract](#) | [Publisher Full Text](#)
49. Cowell IG, Austin CA: **Mechanism of generation of therapy related leukemia in response to anti-topoisomerase II agents.** *Int J Environ Res Public Health*. 2012; **9**(6): 2075–91.
[PubMed Abstract](#) | [Publisher Full Text](#) | [Free Full Text](#)
50. Kenis H, Zandbergen HR, Hofstra L, *et al.*: **Annexin A5 uptake in ischemic myocardium: demonstration of reversible phosphatidylserine externalization and feasibility of radionuclide imaging.** *J Nucl Med*. 2010; **51**(2): 259–67.
[PubMed Abstract](#) | [Publisher Full Text](#)
51. Zurlo J, Arterburn LM: **Characterization of a primary hepatocyte culture system for toxicological studies.** *In Vitro Cell Dev Biol Anim*. 1996; **32**(4): 211–20.
[PubMed Abstract](#) | [Publisher Full Text](#)
52. Downey T: **Analysis of a multifactor microarray study using Partek genomics solution.** *Methods Enzymol*. 2006; **411**: 256–70.
[PubMed Abstract](#) | [Publisher Full Text](#)
53. Ringné M: **What is principal component analysis?** *Nat Biotechnol*. 2008; **26**(3): 303–4.
[PubMed Abstract](#) | [Publisher Full Text](#)
54. Kaushal D, Naeve CW: **An overview of Spotfire for gene-expression studies.** *Curr Protoc Hum Genet*. 2005; **Chapter 11**: Unit 11 9.
[PubMed Abstract](#) | [Publisher Full Text](#)
55. Warde-Farley D, Donaldson SL, Comes O, *et al.*: **The GeneMANIA prediction server: biological network integration for gene prioritization and predicting gene function.** *Nucleic Acids Res*. 2010; **38**(Web Server issue): W214–20.
[PubMed Abstract](#) | [Publisher Full Text](#) | [Free Full Text](#)
56. Zuberi K, Franz M, Rodriguez H, *et al.*: **GeneMANIA prediction server 2013 update.** *Nucleic Acids Res*. 2013; **41**(Web Server issue): W115–22.
[PubMed Abstract](#) | [Publisher Full Text](#) | [Free Full Text](#)
57. Gao C, Cheng X, Lam M, *et al.*: **Signal-dependent regulation of transcription by histone deacetylase 7 involves recruitment to promyelocytic leukemia protein nuclear bodies.** *Mol Biol Cell*. 2008; **19**(7): 3020–7.
[PubMed Abstract](#) | [Publisher Full Text](#) | [Free Full Text](#)
58. Fenech M, Kirsch-Volders M, Natarajan AT, *et al.*: **Molecular mechanisms of micronucleus, nucleoplasmic bridge and nuclear bud formation in mammalian and human cells.** *Mutagenesis*. 2011; **26**(1): 125–32.
[PubMed Abstract](#) | [Publisher Full Text](#)
59. Massagué J: **How cells read TGF-beta signals.** *Nat Rev Mol Cell Biol*. 2000; **1**(3): 169–78.
[PubMed Abstract](#) | [Publisher Full Text](#)
60. Massagué J: **TGF-β signaling in development and disease.** *FEBS Lett*. 2012; **586**(14): 1833.
[PubMed Abstract](#) | [Publisher Full Text](#)
61. Bellomo C, Caja L, Moustakas A: **Transforming growth factor β as regulator of cancer stemness and metastasis.** *Br J Cancer*. 2016; **115**(7): 761–9.
[PubMed Abstract](#) | [Publisher Full Text](#) | [Free Full Text](#)
62. Siegel PM, Massagué J: **Cytostatic and apoptotic actions of TGF-beta in homeostasis and cancer.** *Nat Rev Cancer*. 2003; **3**(11): 807–21.
[PubMed Abstract](#) | [Publisher Full Text](#)
63. Oliner JD, Kinzler KW, Meltzer PS, *et al.*: **Amplification of a gene encoding a p53-associated protein in human sarcomas.** *Nature*. 1992; **358**(6381): 80–3.
[PubMed Abstract](#) | [Publisher Full Text](#)
64. Araki S, Eitel JA, Batuello CN, *et al.*: **TGF-beta1-induced expression of human Mdm2 correlates with late-stage metastatic breast cancer.** *J Clin Invest*. 2010; **120**(1): 290–302.
[PubMed Abstract](#) | [Publisher Full Text](#) | [Free Full Text](#)
65. Lakin ND, Jackson SP: **Regulation of p53 in response to DNA damage.** *Oncogene*. 1999; **18**(53): 7644–55.
[PubMed Abstract](#) | [Publisher Full Text](#)
66. Wade M, Li YC, Wahl GM: **MDM2, MDMX and p53 in oncogenesis and cancer therapy.** *Nat Rev Cancer*. 2013; **13**(2): 83–96.
[PubMed Abstract](#) | [Publisher Full Text](#) | [Free Full Text](#)
67. Gu L, Zhu N, Zhang H, *et al.*: **Regulation of XIAP translation and induction by MDM2 following irradiation.** *Cancer Cell*. 2009; **15**(5): 363–75.
[PubMed Abstract](#) | [Publisher Full Text](#) | [Free Full Text](#)
68. Sun C, Cai M, Gunasekera AH, *et al.*: **NMR structure and mutagenesis of the inhibitor-of-apoptosis protein XIAP.** *Nature*. 1999; **401**(6755): 818–22.
[PubMed Abstract](#) | [Publisher Full Text](#)
69. Chai J, Shiozaki E, Srinivasula SM, *et al.*: **Structural basis of caspase-7 inhibition by XIAP.** *Cell*. 2001; **104**(5): 769–80.
[PubMed Abstract](#) | [Publisher Full Text](#)
70. Huang Y, Park YC, Rich RL, *et al.*: **Structural basis of caspase inhibition by XIAP: differential roles of the linker versus the BIR domain.** *Cell*. 2001; **104**(5): 781–90.
[PubMed Abstract](#) | [Publisher Full Text](#)
71. Riedl SJ, Renatus M, Schwarzenbacher R, *et al.*: **Structural basis for the inhibition of caspase-3 by XIAP.** *Cell*. 2001; **104**(5): 791–800.
[PubMed Abstract](#) | [Publisher Full Text](#)
72. Srinivasula SM, Hegde R, Saleh A, *et al.*: **A conserved XIAP-interaction motif in caspase-9 and Smac/DIABLO regulates caspase activity and apoptosis.** *Nature*. 2001; **410**(6824): 112–6.
[PubMed Abstract](#) | [Publisher Full Text](#)
73. Shiozaki EN, Chai J, Rigotti DJ, *et al.*: **Mechanism of XIAP-mediated inhibition of caspase-9.** *Mol Cell*. 2003; **11**(2): 519–27.
[PubMed Abstract](#) | [Publisher Full Text](#)
74. Richter K, Haslbeck M, Buchner J: **The heat shock response: life on the verge of death.** *Mol Cell*. 2010; **40**(2): 253–66.
[PubMed Abstract](#) | [Publisher Full Text](#)
75. Kampinga HH, Bergink S: **Heat shock proteins as potential targets for protective strategies in neurodegeneration.** *Lancet Neurol*. 2016; **15**(7): 748–59.
[PubMed Abstract](#) | [Publisher Full Text](#)
76. Gozzelino R, Jeney V, Soares MP: **Mechanisms of cell protection by heme oxygenase-1.** *Annu Rev Pharmacol Toxicol*. 2010; **50**: 323–54.
[PubMed Abstract](#) | [Publisher Full Text](#)
77. Han J, Flemington C, Houghton AB, *et al.*: **Expression of bbc3, a pro-apoptotic BH3-only gene, is regulated by diverse cell death and survival signals.** *Proc Natl Acad Sci U S A*. 2001; **98**(20): 11318–23.
[PubMed Abstract](#) | [Publisher Full Text](#) | [Free Full Text](#)
78. Nakano K, Vousden KH: **PUMA, a novel proapoptotic gene, is induced by p53.** *Mol Cell*. 2001; **7**(3): 683–94.
[PubMed Abstract](#) | [Publisher Full Text](#)
79. Mizushima N, Noda T, Yoshimori T, *et al.*: **A protein conjugation system essential for autophagy.** *Nature*. 1998; **395**(6700): 395–8.
[PubMed Abstract](#) | [Publisher Full Text](#)
80. Mizushima N, Komatsu M: **Autophagy: renovation of cells and tissues.** *Cell*. 2011; **147**(4): 728–41.
[PubMed Abstract](#) | [Publisher Full Text](#)
81. Walczak M, Martens S: **Dissecting the role of the Atg12-Atg5-Atg16 complex during autophagosome formation.** *Autophagy*. 2013; **9**(3): 424–5.
[PubMed Abstract](#) | [Publisher Full Text](#) | [Free Full Text](#)
82. Farré JC, Subramani S: **Mechanistic insights into selective autophagy pathways: lessons from yeast.** *Nat Rev Mol Cell Biol*. 2016; **17**(9): 537–52.
[PubMed Abstract](#) | [Publisher Full Text](#)
83. Wang Y, Zhang N, Zhang L, *et al.*: **Autophagy Regulates Chromatin Ubiquitination in DNA Damage Response through Elimination of SQSTM1/p62.** *Mol Cell*. 2016; **63**(1): 34–48.
[PubMed Abstract](#) | [Publisher Full Text](#)
84. Hewitt G, Carroll B, Sarallah R, *et al.*: **SQSTM1/p62 mediates crosstalk between autophagy and the UPS in DNA repair.** *Autophagy*. 2016; **12**(10): 1917–1930.
[PubMed Abstract](#) | [Publisher Full Text](#)
85. Wang Y, Zhu WG, Zhao Y: **Autophagy substrate SQSTM1/p62 regulates chromatin ubiquitination during the DNA damage response.** *Autophagy*. 2017; **13**(1): 212–213.
[PubMed Abstract](#) | [Publisher Full Text](#) | [Free Full Text](#)
86. Vessoni AT, Filippi-Chiela EC, Menck CF, *et al.*: **Autophagy and genomic integrity.** *Cell Death Differ*. 2013; **20**(11): 1444–54.
[PubMed Abstract](#) | [Publisher Full Text](#) | [Free Full Text](#)
87. Hewitt G, Korolchuk VI: **Repair, Reuse, Recycle: The Expanding Role of Autophagy in Genome Maintenance.** *Trends Cell Biol*. 2016; pii: S0962-8924(16)30209-4.
[PubMed Abstract](#) | [Publisher Full Text](#)
88. Settembre C, Fraldi A, Medina DL, *et al.*: **Signals from the lysosome: a control centre for cellular clearance and energy metabolism.** *Nat Rev Mol Cell Biol*. 2013; **14**(5): 283–96.
[PubMed Abstract](#) | [Publisher Full Text](#) | [Free Full Text](#)
89. Desdín-Micó G, Mittelbrunn M: **Role of exosomes in the protection of cellular homeostasis.** *Cell Adh Migr*. 2016; 1–8.
[PubMed Abstract](#) | [Publisher Full Text](#)
90. Papandreou ME, Tavernarakis N: **Autophagy and the endo/exosomal pathways in health and disease.** *Biotechnol J*. 2017; **12**(1).
[PubMed Abstract](#) | [Publisher Full Text](#)
91. Ferrara N, Gerber HP, LeCouter J: **The biology of VEGF and its receptors.** *Nat Med*. 2003; **9**(6): 669–76.
[PubMed Abstract](#) | [Publisher Full Text](#)
92. Simons M, Gordon E, Claesson-Welsh L: **Mechanisms and regulation of endothelial VEGF receptor signalling.** *Nat Rev Mol Cell Biol*. 2016; **17**(10): 611–25.
[PubMed Abstract](#) | [Publisher Full Text](#)
93. Babapoor-Farrokhran S, Jee K, Puchner B, *et al.*: **Angiopoietin-like 4 is a potent angiogenic factor and a novel therapeutic target for patients with proliferative diabetic retinopathy.** *Proc Natl Acad Sci U S A*. 2015; **112**(23): E3030–9.
[PubMed Abstract](#) | [Publisher Full Text](#) | [Free Full Text](#)
94. Guo L, Li SY, Ji FY, *et al.*: **Role of Angptl4 in vascular permeability and inflammation.** *Inflamm Res*. 2014; **63**(1): 13–22.
[PubMed Abstract](#) | [Publisher Full Text](#)

95. Gacche RN: **Compensatory angiogenesis and tumor refractoriness.** *Oncogenesis*. 2015; **4**(6): e153.
[PubMed Abstract](#) | [Publisher Full Text](#) | [Free Full Text](#)
96. Nabeshima K, Inoue T, Shimao Y, *et al.*: **Matrix metalloproteinases in tumor invasion: role for cell migration.** *Pathol Int*. 2002; **52**(4): 255–64.
[PubMed Abstract](#) | [Publisher Full Text](#)
97. Bonnans C, Chou J, Werb Z: **Remodelling the extracellular matrix in development and disease.** *Nat Rev Mol Cell Biol*. 2014; **15**(12): 786–801.
[PubMed Abstract](#) | [Publisher Full Text](#) | [Free Full Text](#)
98. Paul CD, Mistriotis P, Konstantopoulos K: **Cancer cell motility: lessons from migration in confined spaces.** *Nat Rev Cancer*. 2017; **17**(2): 131–140.
[PubMed Abstract](#) | [Publisher Full Text](#)
99. Mittal R, Patel AP, Debs LH, *et al.*: **Intricate Functions of Matrix Metalloproteinases in Physiological and Pathological Conditions.** *J Cell Physiol*. 2016; **231**(12): 2599–621.
[PubMed Abstract](#) | [Publisher Full Text](#)
100. Steeg PS: **Targeting metastasis.** *Nat Rev Cancer*. 2016; **16**(4): 201–18.
[PubMed Abstract](#) | [Publisher Full Text](#)
101. Eming SA, Martin P, Tomic-Canic M: **Wound repair and regeneration: mechanisms, signaling, and translation.** *Sci Transl Med*. 2014; **6**(265): 265sr6.
[PubMed Abstract](#) | [Publisher Full Text](#) | [Free Full Text](#)
102. Buschbeck M, Hake SB: **Variants of core histones and their roles in cell fate decisions, development and cancer.** *Nat Rev Mol Cell Biol*. 2017.
[PubMed Abstract](#) | [Publisher Full Text](#)
103. Hammond CM, Strømme CB, Huang H, *et al.*: **Histone chaperone networks shaping chromatin function.** *Nat Rev Mol Cell Biol*. 2017.
[PubMed Abstract](#) | [Publisher Full Text](#)
104. Talbert PB, Henikoff S: **Histone variants on the move: substrates for chromatin dynamics.** *Nat Rev Mol Cell Biol*. 2017; **18**(2): 115–126.
[PubMed Abstract](#) | [Publisher Full Text](#)
105. Kari R, Chung HR, Lasserre J, *et al.*: **Histone modification levels are predictive for gene expression.** *Proc Natl Acad Sci U S A*. 2010; **107**(7): 2926–31.
[PubMed Abstract](#) | [Publisher Full Text](#) | [Free Full Text](#)
106. Jin J, Cai Y, Li B, *et al.*: **In and out: histone variant exchange in chromatin.** *Trends Biochem Sci*. 2005; **30**(12): 680–7.
[PubMed Abstract](#) | [Publisher Full Text](#)
107. Hauer MH, Seeber A, Singh V, *et al.*: **Histone degradation in response to DNA damage enhances chromatin dynamics and recombination rates.** *Nat Struct Mol Biol*. 2017.
[PubMed Abstract](#) | [Publisher Full Text](#)
108. Matsuda S, Rouault J, Magaud J, *et al.*: **In search of a function for the TIS21/PC3/BTG1/TOB family.** *FEBS Lett*. 2001; **497**(2–3): 67–72.
[PubMed Abstract](#) | [Publisher Full Text](#)
109. Winkler GS: **The mammalian anti-proliferative BTG/Tob protein family.** *J Cell Physiol*. 2010; **222**(1): 66–72.
[PubMed Abstract](#) | [Publisher Full Text](#)
110. Gartel AL, Radhakrishnan SK: **Lost in transcription: p21 repression, mechanisms, and consequences.** *Cancer Res*. 2005; **65**(10): 3980–5.
[PubMed Abstract](#) | [Publisher Full Text](#)
111. Cazzalini O, Scovassi AI, Savio M, *et al.*: **Multiple roles of the cell cycle inhibitor p21^{CDKN1A} in the DNA damage response.** *Mutat Res*. 2010; **704**(1–3): 12–20.
[PubMed Abstract](#) | [Publisher Full Text](#)
112. Muñoz-Espín D, Serrano M: **Cellular senescence: from physiology to pathology.** *Nat Rev Mol Cell Biol*. 2014; **15**(7): 482–96.
[PubMed Abstract](#) | [Publisher Full Text](#)
113. Tomasini R, Seux M, Nowak J, *et al.*: **TP53INP1 is a novel p73 target gene that induces cell cycle arrest and cell death by modulating p73 transcriptional activity.** *Oncogene*. 2005; **24**(55): 8093–104.
[PubMed Abstract](#) | [Publisher Full Text](#)
114. Azam N, Vairapandi M, Zhang W, *et al.*: **Interaction of CR6 (GADD45gamma) with proliferating cell nuclear antigen impedes negative growth control.** *J Biol Chem*. 2001; **276**(4): 2766–74.
[PubMed Abstract](#) | [Publisher Full Text](#)
115. Niehrs C, Schäfer A: **Active DNA demethylation by Gadd45 and DNA repair.** *Trends Cell Biol*. 2012; **22**(4): 220–7.
[PubMed Abstract](#) | [Publisher Full Text](#)
116. Ohshima Y, Okada N, Tani T, *et al.*: **Nucleotide sequences of mouse genomic loci including a gene or pseudogene for U6 (4.8S) nuclear RNA.** *Nucleic Acids Res*. 1981; **9**(19): 5145–58.
[PubMed Abstract](#) | [Publisher Full Text](#) | [Free Full Text](#)
117. Wu JA, Manley JL: **Base pairing between U2 and U6 snRNAs is necessary for splicing of a mammalian pre-mRNA.** *Nature*. 1991; **352**(6338): 818–21.
[PubMed Abstract](#) | [Publisher Full Text](#)
118. Datta B, Weiner AM: **Genetic evidence for base pairing between U2 and U6 snRNA in mammalian mRNA splicing.** *Nature*. 1991; **352**(6338): 821–4.
[PubMed Abstract](#) | [Publisher Full Text](#)
119. Yean SL, Wuenschell G, Termini J, *et al.*: **Metal-ion coordination by U6 small nuclear RNA contributes to catalysis in the spliceosome.** *Nature*. 2000; **408**(6814): 881–4.
[PubMed Abstract](#) | [Publisher Full Text](#) | [Free Full Text](#)
120. Krämer A, Green J, Pollard J Jr, *et al.*: **Causal analysis approaches in Ingenuity Pathway Analysis.** *Bioinformatics*. 2014; **30**(4): 523–30.
[PubMed Abstract](#) | [Publisher Full Text](#) | [Free Full Text](#)
121. Lamb J, Crawford ED, Peck D, *et al.*: **The Connectivity Map: using gene-expression signatures to connect small molecules, genes, and disease.** *Science*. 2006; **313**(5795): 1929–35.
[PubMed Abstract](#) | [Publisher Full Text](#)
122. Lamb J: **The Connectivity Map: a new tool for biomedical research.** *Nat Rev Cancer*. 2007; **7**(1): 54–60.
[PubMed Abstract](#) | [Publisher Full Text](#)
123. Fuchs Y, Steller H: **Live to die another way: modes of programmed cell death and the signals emanating from dying cells.** *Nat Rev Mol Cell Biol*. 2015; **16**(6): 329–44.
[PubMed Abstract](#) | [Publisher Full Text](#) | [Free Full Text](#)
124. Kruijswijk F, Labuschagne CF, Vousden KH: **p53 in survival, death and metabolic health: a lifeguard with a licence to kill.** *Nat Rev Mol Cell Biol*. 2015; **16**(7): 393–405.
[PubMed Abstract](#) | [Publisher Full Text](#)
125. Wang J, Zhang J, Lee YM, *et al.*: **Quantitative chemical proteomics profiling of de novo protein synthesis during starvation-mediated autophagy.** *Autophagy*. 2016; **12**(10): 1931–1944.
[PubMed Abstract](#) | [Publisher Full Text](#) | [Free Full Text](#)
126. Füllgrabe J, Klionsky DJ, Joseph B: **The return of the nucleus: transcriptional and epigenetic control of autophagy.** *Nat Rev Mol Cell Biol*. 2014; **15**(1): 65–74.
[PubMed Abstract](#) | [Publisher Full Text](#)
127. Hetz C: **The unfolded protein response: controlling cell fate decisions under ER stress and beyond.** *Nat Rev Mol Cell Biol*. 2012; **13**(2): 89–102.
[PubMed Abstract](#) | [Publisher Full Text](#)
128. Narula J, Haider N, Arbustini E, *et al.*: **Mechanisms of disease: apoptosis in heart failure—seeing hope in death.** *Nat Clin Pract Cardiovasc Med*. 2006; **3**(12): 681–8.
[PubMed Abstract](#) | [Publisher Full Text](#)
129. Tang HL: **Reversal of apoptosis: a potential link to carcinogenesis and cancer recurrence.** (CUHK, CUHK electronic theses & dissertations collection, 2010).
[Reference Source](#)

Open Peer Review

Current Referee Status:   

Version 2

Referee Report 10 March 2017

doi:[10.5256/f1000research.11669.r19460](https://doi.org/10.5256/f1000research.11669.r19460)



Leonard K. Kaczmarek

Department of Pharmacology, Yale School of Medicine, New Haven, CT, USA

The data presented build on the authors' earlier studies of reversal of apoptosis. They provide useful information documenting changes in gene expression following 5 hours of exposure to ethanol, an apoptotic stimulus to primary mouse liver cells. The findings only make sense when taken in combination with the authors previous work, which provides a compelling case that the recovery from apoptosis is indeed occurring, and the manuscript documents some of this by reprinting figure panels from an earlier publication in Figure 1.

My only minor comment is that, at least in some cells such as neurons, cleavage of caspase-3 can be a regulatory signal that does not herald cell death, but may influence biological processes such as synaptic function.

I have read this submission. I believe that I have an appropriate level of expertise to confirm that it is of an acceptable scientific standard.

Competing Interests: No competing interests were disclosed.

Referee Report 10 February 2017

doi:[10.5256/f1000research.11669.r20082](https://doi.org/10.5256/f1000research.11669.r20082)



Takafumi Miyamoto

University of Tokyo, Tokyo, Japan

The authors sincerely responded to my comment with deep consideration. Therefore I have no objection to this article being indexed.

I have read this submission. I believe that I have an appropriate level of expertise to confirm that it is of an acceptable scientific standard.

Competing Interests: No competing interests were disclosed.

Version 1

Referee Report 30 January 2017

doi:10.5256/f1000research.11388.r19503



Sanzhen Liu

Department of Plant Pathology, Kansas State University, Manhattan, KS, USA

The manuscript by Tang et al. was focused on the elucidation of the molecular mechanisms of an important phenomenon, anastasis, through time-course expression profiling. Anastasis was recently discovered and has not been fully studied yet. Its molecular basis remains to be uncovered. The study provided useful information to better understand this underexplored process. Overall, the experiment was well designed. The time course experiment included six time points, untreated samples as the control, toxin-induced apoptosis, and four time points after removal of toxin. Three biological replicates were performed at each time point. Figure 1 illustrated the experimental design very well. The biological interpretation of microarray results is reasonable. The reviewer has no major concerns. However, several minor changes are needed, especially for the presentation of figures, which could be improved.

First, no multiple test correction was mentioned in the microarray analysis section. It was described that the p-value less than 0.05 was used to declare statistical significance. The reviewer would suggest the authors confirm that. A false discovery rate (FDR) method is needed for multiple test correction.

Second, the PCA result from Figure 2A showed that three biological replicates were closely clustered, which showed a good repeatability. However, the goal of PCA is not just check the repeatability of three replicates of each group (time point). PCA can be also used to examine the relationship among groups. My recommendation is that the authors provide more description for the PCA result. In addition, in Figure 2A, the percentage of PC2 explaining total variation was masked. But based on the value of PC3, it should be greater than 5.89%. Given the high value of PC1, I would suggest plotting a two dimension PCA plot to display the result or re-plotting this three-dimension plot.

Third, it would be useful to list the number of significant differential expression for each comparison. And I guess the clustering result in Figure 3 presented all significant genes.

Figure 4 showed some interesting result about gene interactions. I did not see enough description about this figure in the main text.

Editorial comments:

In the Abstract, "whole genome" can be replaced by "genome-wide".

I have read this submission. I believe that I have an appropriate level of expertise to confirm that it is of an acceptable scientific standard.

Competing Interests: No competing interests were disclosed.

Referee Report 20 January 2017

doi:10.5256/f1000research.11388.r19354



Takafumi Miyamoto

University of Tokyo, Tokyo, Japan

This study unravels the gene regulatory network that seems to be involved in the process of anastasis. It is interesting that the authors found various genes that appear to participate in ethanol-induced anastasis, suggesting that the dynamic reconstitution of gene regulatory networks might be a prerequisite for rescuing cells from the brink of cell death. Overall, this work is worth being indexed. However, I would like to see the following points in the research addressed, before approval:

1. Anastasis is a developing concept rather than an established one. It would be better to show the expression dynamics of caspase-3, PARP, and ICAD at all analyzed time points (Cont, R0, R3, R6, R24, and R48). In addition, why don't the authors show apoptotic DNA fragmentation to make sure that all the analyzed cells in the anastasis stage definitely underwent apoptosis?
2. I may have missed noting this, but there is no statistical analysis of the gene expression changes observed in the microarray data. In Fig. 2B, the expression levels of several genes seem different in the same time point replicates. It would be better to show the genes that were induced or suppressed during anastasis, along with the statistical significance of the differences.
3. Given the importance of understanding the mechanism of anastasis, it would be better to verify the data obtained from microarray analysis, by using quantitative PCR or Western blotting.

I have read this submission. I believe that I have an appropriate level of expertise to confirm that it is of an acceptable scientific standard, however I have significant reservations, as outlined above.

Competing Interests: No competing interests were disclosed.

Author Response 03 Feb 2017

Ho Lam Tang, Johns Hopkins University, USA

We thank for the enthusiasm and valuable input from the reviewer, and have made the following changes:

1. We have included the Western blot data (Figure 1B), which shows that caspase-3, PARP and ICAD were cleaved during apoptosis, but then recovered to their original level at 24 hours after removal of the cell death stimulus. Interestingly, our microarray data shows that their level of mRNA remained no significant change at all time points (3, 6, 24 and 48 hours) after removal of the cell death stimulus, compared with the untreated (control) cells (data available at figshare, please see *Data availability* in the manuscript), suggesting the recovery of corresponding proteins is contributed by the regulation of translation during and after anastasis. The related data and discussion are included in our revised manuscript.

Our earlier studies using time-lapse live cell microscopy and comic assay demonstrated that the current apoptotic induction (4.5% ethanol, 5 hours) can trigger DNA damage. After removal of the stimulus, major of the dying cells can recover. Interestingly, some cells that reversed apoptosis display chromosomal abnormality and oncogenic transformation, indicating reversibility of apoptosis after DNA damage. In our current study, we further found significant reduction of mRNA level of multiple histone genes during anastasis. Notably, cellular levels of histones reduce in response to DNA damage, as to enhance DNA repairing. Therefore, reduction of expression of histones during anastasis could be a sign of

cells that recover from DNA damage after apoptosis.

2. We have included supplementary data with corresponding p-value for statistical significance of fold change for all of the 3 biological replicants of each gene (see Data availability). The software for the microarray data analysis is mentioned at the “Materials and methods” section.
3. We have verified our data by RT-PCR in human liver cancer HepG2 cell line, and included the data in the new Figure 4.

Competing Interests: No competing interests were disclosed.
